



NGST Payload Study

General Design Considerations

NGST – DSS – WHRP – 001

October 1, 1999

Work performed under ESA contract for the
“Study of Payload Suite and Telescope for NGST”
ESTEC/Contract no. 13111/98/NL/MS

Table of Contents

1	INTRODUCTION.....	3
2	GENERAL DESIGN CONSIDERATIONS	5
2.1	OPTICAL SYSTEM DESIGN AND INTERFACE PHILOSOPHY.....	5
2.1.1	<i>Instrument Design Philosophy.....</i>	5
2.1.2	<i>Optical Interface to Telescope.....</i>	5
2.1.3	<i>Optical Material Trades</i>	6
2.2	MECHANICAL DESIGN CONSIDERATIONS.....	7
2.2.1	<i>Material Trade-Off.....</i>	7
2.2.2	<i>Mechanisms</i>	12
2.2.3	<i>Mechanical Interfaces</i>	14
2.3	THERMAL DESIGN, ANALYSIS AND COOLING CONCEPTS.....	15
2.3.1	<i>Thermal Requirements and Constraints</i>	15
2.3.2	<i>Thermal Design and Heat Load Budget of NIR Instruments</i>	16
2.3.3	<i>Passive Cooling Concept for NIR Instruments</i>	18
2.3.4	<i>Thermal Design and Heat Load Budget of MIR Instruments</i>	19
2.3.5	<i>Cooling Concepts for MIR Instruments.....</i>	23
2.4	DETECTORS.....	30
2.4.1	<i>Near Infrared (NIR) Detectors</i>	30
2.4.2	<i>Mid Infrared Detectors.....</i>	34
2.4.3	<i>Detector Performance Summary</i>	37
2.5	ELECTRICAL DESIGN.....	39
2.5.1	<i>Instrument Electrical System Overview.....</i>	39
2.5.2	<i>Analog Signal Processing Design Trades</i>	44
2.5.3	<i>FPU Readout Scheme.....</i>	47
2.5.4	<i>Signal Processing Power Budget and Harness Size.....</i>	49
2.6	SIGNAL PROCESSING.....	51
2.6.1	<i>Up-the-ramp sampling:</i>	51
2.6.2	<i>NIRCAM FTS Signal Processing.....</i>	53
2.6.3	<i>Data Processing Requirements.....</i>	53
2.7	CRITICAL AREAS AND RECOMMENDED DEVELOPMENT ACTIVITIES	56
2.7.1	<i>Generic Instrument Hardware Breakdown.....</i>	56
2.7.2	<i>Critical Areas and Technology Requirements</i>	56
2.7.3	<i>Recommended Development Activities</i>	58
2.7.4	<i>Technology Development Roadmap</i>	59
2.8	DEVELOPMENT PLANNING FOR PHASES B AND C/D	60
3	REFERENCES.....	61

1 INTRODUCTION

As part of its Origins program, NASA is currently undertaking definition and feasibility studies of a Next Generation Space Telescope (NGST) to succeed the Hubble Space Telescope (HST) after 2005. NGST is foreseen to have an aperture of 8 meters and be optimized for near infrared wavelengths (0.6 - 10+ microns) in order to enable the exploration of the most remote high redshift universe.

NASA has invited ESA to extend their successful collaboration on HST to the NGST project, and a draft agreement concept is in place which aims at securing European participation in NGST at a similar level as on HST. ESA has undertaken a number of assessment studies which aimed at defining its potential instrument and spacecraft hardware contributions to the mission.

One of these ESA studies called "Study of Payload Suite and Telescope for NGST" (ref. /1/), has been conducted by Dornier Satellitensysteme GmbH (DSS), Ottobrunn, together with Alcatel Space (AS), Cannes, and a team of 16 European science institutes chaired by Laboratoire d'Astronomie Spatiale, Marseille, and UK Astronomy Technology Centre, Edinburgh. DSS took the responsibility for the overall study and the payload, AS for the telescope, and the science team was responsible for the instrument and telescope definition and requirements.

The four potential NGST instruments that have been studied under this contract are

- NIRCAM – Filter Wheel (NGST-DSS-WHRP-002)
- NIRCAM – Imaging FTS (NGST-DSS-WHRP-003)
- MIRCAM (NGST-DSS-WHRP-004, together with MIRIFS)
- MIRIFS

The instrument opto-mechanical designs and analyses of these instruments as well as the instrument specific development planning are discussed in the indicated reports.

This documents deals with technical aspects that are common to all payloads studied by DSS. This includes also the IFMOS (NIR integral field spectrograph), which has been studied under CNRS sub-contract in a different NGST study (ref. /3/).

The technical aspects discussed in this document include

- optical interface
- material selection, mechanisms
- thermal design and analysis
- electrical design, detectors, data processing
- common critical areas

Payload Study Team

ESA:

NGST study manager

J. Cornelisse

NGST study scientist

Dr. P. Jakobsen

Dornier Satellitensysteme:

Study mgmt., system engineering

W. Posselt

Optical engineering

Dr. W. Holota, P. de Zoeten

Mechanical engineering

D. Scheulen, H. Huether

Thermal engineering

A. Hauser

Electrical eng., data processing

W. Hupfer

Focal plane arrays

Dr. R. Buschner-Ueberreiter

2 GENERAL DESIGN CONSIDERATIONS

2.1 Optical System Design and Interface Philosophy

2.1.1 *Instrument Design Philosophy*

The instrument optical system and interface design philosophy is embedded into the overall NGST development philosophy, which requires a short development period and an adapted model philosophy.

In view of the schedule constraints the emphasis on the instrument concept selection and design detailing has been on

- low complexity
- low criticality, based on experience as far as possible
- simple design and manufacturing
- simple alignment and testing

with acceptable compromises on

- budgets
- performance

The instrument designs that have evolved during the payload study are considered a good compromise between these conflicting requirements.

2.1.2 *Optical Interface to Telescope*

Pre-requisite for the telescope and instrument conceptual design activities was the agreement on the common interface. This interface is defined by the telescope focal plane, for which the following considerations have been made:

- *The optical beam interface should be telecentric and flat across the telescope focal plane.*

Such an interface will have the following advantages:

- + simple instrument design
- + insensitive to instrument re-location during development phase
- + eases instrument alignment and testing facilities

These interface requirements will increase the effort and budgets of the telescope. Therefore, the actual telescope design that evolved in the course of the study is a compromise and provides a quasi-telecentric interface, i.e. the difference between the ideal interface is negligible for small field angles.

- *The telescope f-number should be $f/D = 16$*

The instrument size is mainly determined by the detector pixel size. Therefore, the smallest available detector pixels (18.5 μm pitch) should be selected for the wide field NIR camera, and the telescope f-number be adapted accordingly. This will ensure

+ minimum instrument and payload suite mass and dimensions

(Note: recent considerations about the MTF of small detector pixels suggest a somewhat increased f-number as a better compromise between performance and instrument budgets.)

Summary: the instrument designs are all based on the assumption of a telescope f-number of 16 and a telecentric and flat field optical interface at the telescope focal plane.

2.1.3 Optical Material Trades

The available types of optical materials for IR instruments can be characterized as reflective or refractive or hybrid solutions. Use of *reflective optics* is preferred mainly because of its suitability for a large wavelength range and its low criticality under space environment.

The main advantages and disadvantages of reflective optical elements are summarized below:

- + achromatic (wavelength independent)
- + lower temperature criticality (if material CTE matches structure)
- + lower sensitivity to mechanical loads (launch)
- + no gluing (as for transmission filters)
- + insensitive to radiation environment
- increased dimensions of optics and instrument (or reduction of instrument field)
- requires better surface accuracy

2.2 Mechanical Design Considerations

The structural instrument designs aim for low criticality during all MAIT steps.

The natural choice for the structure of each of the four instruments is an optical bench carrying the optical components in a 2D configuration. Such an arrangement provides design flexibility, high thermal stability, good accessibility of the optical components and allows sequential assembly and adjustment.

2.2.1 Material Trade-Off

Material Requirements

For the NGST operating conditions the following specific material requirements have been identified:

- low Coefficient of Thermal Expansion (CTE) at RT and down to 30K

A small CTE will induce small distortions during cool down to 30 K, which are easier to compensate. This reduces complexity, mass and cost. Variations in CTE by material in-homogeneity are smaller in absolute values for a smaller CTE.

- CTE compatibility to optical components (mirrors)

CTE compatibility of the structure and optical components will avoid stress and thermal deformations when cooling down to operational temperature. A larger CTE mismatch will lead either to difficult support designs or to the necessity of active compensation devices.

- high thermal conductivity at RT and at 30 K

A high thermal conductivity of the structure material reduces thermal gradients and corresponding thermal deformations.

- hardness of I/F's

Structural hardness of the material is of advantage for defined and repeatable junctions and interfaces.

In addition general requirements for space materials apply as listed below:

- | | | |
|------------------------|-------------------------------|--------------------------|
| - low specific weight | - homogeneous properties (3D) | - flexibility in shaping |
| - high Young's modulus | - low variation of properties | - good availability |
| - high strength | - easy to manufacture/machine | - low cost |
| - low outgasing | - low toxicity | |

Material Data

The following materials have been considered for the instrument structure, the optical components and the interfaces. Their properties are discussed in the subsequent section.

	spec. Weight	Young's Modulus	CTE at 293 K	CTE at 30 K	therm. Conductivity at 293 K at 30 K	
	g/cm ³	MPa	10 ⁻⁶ /K	10 ⁻⁶ /K	W/m/K	W/m/K
Invar	8.1	210 000	1.4	0.3	13.5	
Al (alloy)	2.7	70 000	24	1.5	150	30
Al 99.999					237	5180
Beryllium	1.9	300 000	12	0.1	180	100
SiC	2.9	311 000	2.57		156	
C/SiC	2.7	230 000	2.3	0.2	125	
CFRP	1.6	110 000	0.1	0.2 (at 100K)	50	0.1 to 10
Zerodur	2.2	70 000	0.03	-0.7	1.3	

Figure 2.2-1: Physical data of possible structure materials

Material Discussion

INVAR, pure Aluminum, SiC, Zerodur and CFRP are not considered suitable materials for the instrument structure. Their characteristics are only briefly summarized:

Invar

- too heavy for the whole structure
 - long term variation of material properties (CTE) possible (already observed)
- ⇒ only for local applications (small brackets, flexures)

Aluminum 99.999

- too low elastic strength: danger of permanent deformations under launch loads
 - too weak: difficult to machine and no hard I/F possible
 - excellent thermal conductivity
- ⇒ only for local applications (thermal conductor)

SiC

- brittle fracture behavior

- difficult manufacturing processes (raw material production and machining); low flexibility in shaping, especially for larger components
 - expensive (manufacturing and machining)
- ⇒ not suited for the structure, but possible candidate for the mirrors

Zerodur

- brittle and crack sensitive material
 - difficult manufacturing processes (raw material production and machining); low flexibility in shaping
 - bad thermal conductivity
 - relatively high (negative) CTE at 30 K
 - expensive (manufacturing and machining)
- ⇒ not suited for the structure; but eventually for the mirrors

CFRP

- orthotropic 3D properties: optimization only in one or two directions possible
 - difficult to achieve a 3D thermally stable design in tight complex structures
 - relatively bad thermal conductivity
 - moisture desorption is critical (only one direction can be tailored to Zero: e.g. tubes)
 - no defined and hard I/F surface (needs metallic fittings, where the junction is critical down to 30 K)
- ⇒ not suited for the instruments structure due to the complex (3D) structure needed

The remaining materials **Aluminum**, **Beryllium** and **C/SiC** are realistic candidates for the instrument structure. Therefore, a more detailed discussion of the specific advantages and disadvantages is given:

Aluminum (alloy)

Advantages

- + high thermal conductivity at RT
- + easy to machine
- + high flexibility in shaping
- + good availability
- + low procurement and parts manufacturing costs

Disadvantages

- very high CTE (cool down from 293 to 30K results in 4.1mm shrinkage per 1m structure)
- very high sensitivity to thermal gradients (a thermal gradient of $\pm 5K$ at 30K results in a 7.5 μ m distortion per 1m structure)

- commercially available raw materials (blocks, plates) show variations in 3D properties (\Rightarrow differences in CTE are critical due to the high absolute value)
- low Young's modulus (compared to Be and C/SiC)
- low thermal conductivity at 30 K

Beryllium

Advantages

- + low specific weight
- + very high Young's modulus
- + high thermal conductivity at 30 K
- + flexibility in shaping
- + CTE compatibility with mirrors (assuming Be mirrors)
- + low CTE at 30 K (low sensitivity to thermal variations and thermal gradients)

Disadvantages

- high CTE (cool down from 293 to 30 K results in 1.3mm shrinkage per 1m structure)
- due to the toxicity significant restrictions for raw part machining, assembly and modifications
- limited availability
- high cost (raw material, part manufacturing, assembly and tests)

C/SiC

Advantages

- + high Young's modulus
- + low CTE (cool down from 293 to 30K results in 0.2mm shrinkage per 1m structure; a thermal gradient of ± 5 K at 30 K results in 1 μ m distortion per 1m structure)
- + homogeneous 3D properties
- + high flexibility in shaping
- + high material hardness (precise I/F's possible)
- + CTE compatibility with mirrors (assuming SiC or C/SiC mirrors)
- + medium cost (procurement and parts manufacturing)

Disadvantages

- brittle fracture behavior
- limited availability

Material Selection

The decisive argument for the material choice is the requirement to provide a CTE as low as possible for the mirrors and the connecting structure in view of the large temperature change during cool down from RT to 30 K. It is rather difficult to predict the thermally induced deformations of the different mirror shells if they are made of a material with large CTE like Al or Be. In addition, Al mirrors need a special coating and will have a relatively high CTE even at 30 K, and corresponding high sensitivity to thermal gradients. The CTE of Be is lower, but when selected as material for the structure it should consequently be selected also for all other components (mirrors, brackets, fittings, etc.) with corresponding disadvantages on other fields like toxicity, availability, cost, etc.

Another potential advantage comes from the characteristic of the CTE curve, shown in Figure 2.2-2 below: since the CTE takes slightly negative values in the range from about 70K to 140K, the integral taken from 30K to about 150K will vanish, i.e. the instrument is expected to have the final operational dimensions/shape already at a much higher temperature of about 150K. This can significantly reduce the costs for alignment and testing.

Therefore, C/SiC is the selected baseline material for the instrument structure and the mirrors.

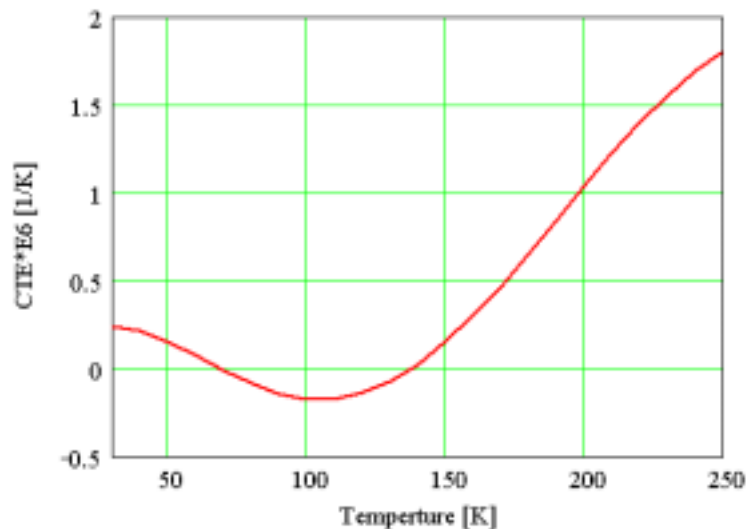


Figure 2.2-2: CTE variation with temperature

2.2.2 Mechanisms

Filter Wheel Mechanism

The proposed design concept for the filter wheel mechanisms is derived from the ISOPHOT filter wheel (see Figure 2.2-2 and Figure 2.2-3).

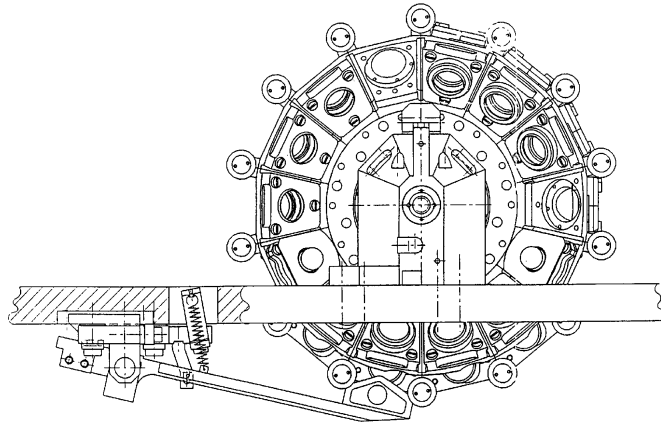


Figure 2.2-3: ISOPHOT filter wheel (side view)

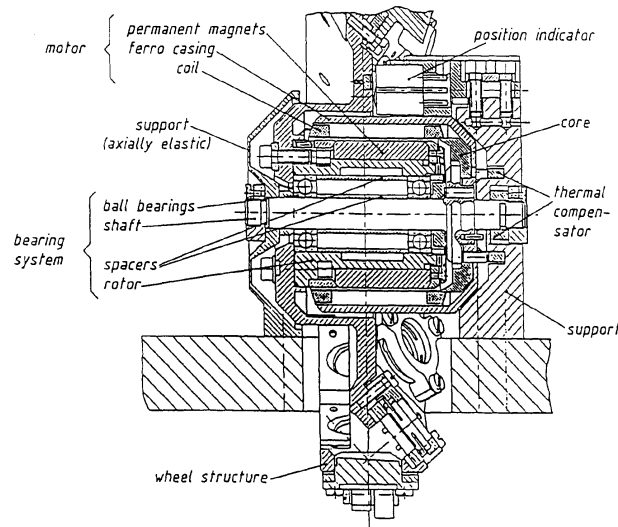


Figure 2.2-4: ISOPHOT filter wheel (section)

Inside the wheel flange a stepper motor is positioned. For every filter change one step is performed, a half step for acceleration and a half step for deceleration. The positioning is secured via a dent by a spring induced centering between ball bearings.

Position sensors are included. Since the wheel is perfectly balanced, no launch lock is needed. The actual position after launch is detected by sensors.

The ISOPHOT filter wheel has a diameter of 110 mm and is operating at 4 K. The dissipation of the mechanism during filter change is 4 mWs per step. In non operating condition the dissipation is zero. For larger filter wheels the dissipation per step will increase approximately quadratic with the wheel diameter.

Refocus Mechanism

As refocusing actuator for the different instruments either a sequential working linear inchworm type is foreseen, which is currently under development for NGST at Burleigh Instruments, or a linear actuator from Rubicon. (Note: no dedicated European development is foreseen, and the final actuator selection will depend on the selected actuator for the telescope M1 adjustment and control.)

The essential actuator data for the inchworm type are a resolution better than 20 nm, a stroke larger than 6 mm, a holding force about 4.5 N, a heat dissipation of 5 mW during calibration and of 0.05 mW during operation. The size of the prototype is about 50 x 50 x 100 mm. The Rubicon actuator has similar performance and budget data.

Hold Down and Release Mechanism

Due to the limited holding force of the linear actuators hold down and release mechanisms have to be foreseen for the refocusing mirrors. The principle of such a mechanism is shown in Figure 2.2-4. During launch the mirror support frame is fixed by a latch with conical stud. After launch the release is actuated via toggle by a gearmotor connected to an eccentric pulley. After release the mirror is completely free. The mechanism works without pyro-techniques and has no dissipation in power-off condition. The gear motor is redundant and combines low mass with high torque.

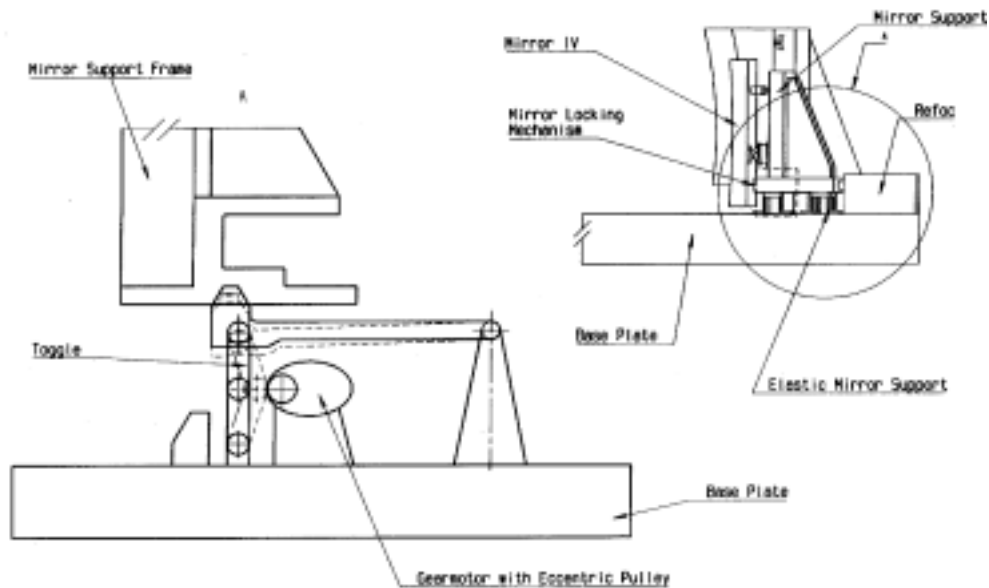


Figure 2.2-5: Hold down and release mechanism for refocusing mirrors

2.2.3 Mechanical Interfaces

The instrument interface to the ISIM will be realized by isostatic mounting to decouple the deformations between the connected structures (Figure 2.2-5). Favorite materials for the flexible mounts are INVAR, titanium or CFRP (the choice will be dependent on the magnitude of the loads and deformations).

The optical components will be mounted in the same way (Figure 2.2-6):

- large mirrors will be fixed by isostatic 3-point-mounting with flexible INVAR mounts
- small mirrors will be fixed by a slotted central INVAR tube

The refocusing mechanism design principle, which tolerates only one degree of freedom, is shown as well.

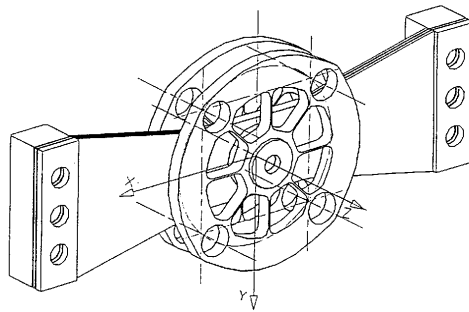


Figure 2.2-6: Design example of flexible interface mount

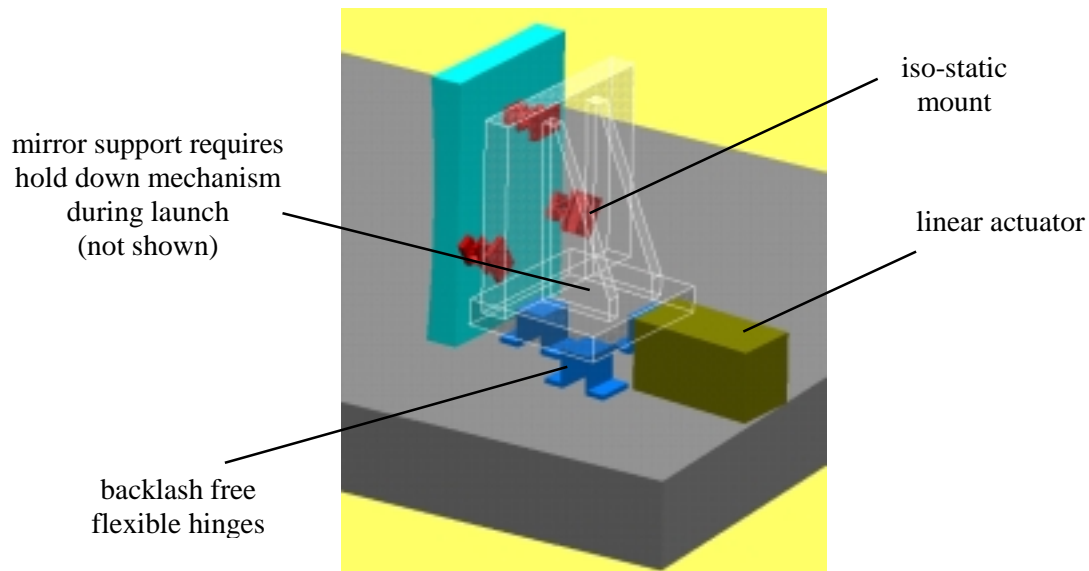


Figure 2.2-7: Iso-static mirror mounting and refocusing mechanisms

2.3 Thermal Design, Analysis and Cooling Concepts

2.3.1 Thermal Requirements and Constraints

Thermal Environment and Specifications

The NGST orbit is at the Lagrangian point L2 at a distance of 1500 000 km in anti-sun direction from the earth. This orbit provides an excellent cooling capability by a passive radiator cooling system: the ISIM will be prevented from solar and earth radiation by a 14 m x 32.8 m sunshield and thermally isolated from the warmer SSM by a 3.75 m thermal insulating truss, see Figure 2.3-1. The temperature of the sunshield shade side is 90 K. A lifetime of 5 years is required, however 10 years are aspired as goal.

The following preliminary thermal requirements are given for the ISIM:

ISIM temperature: 30 K - 50 K

ISIM total heat load: < 200 mW (TBC)

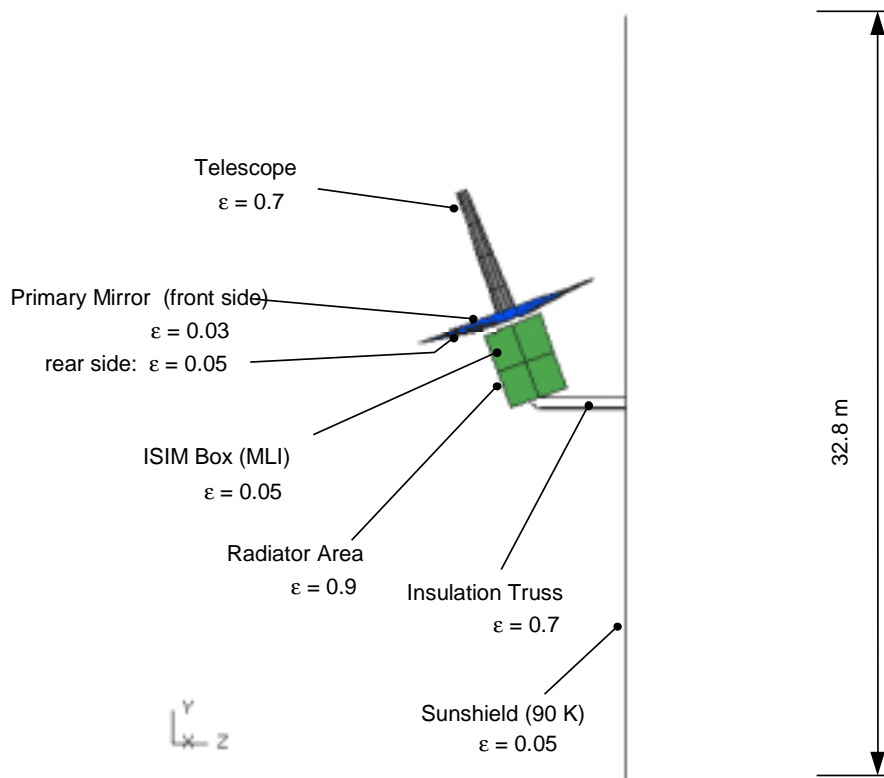


Figure 2.3-1: Thermal characteristics of NGST

Temperature and Estimated Dissipation of ISIM Instruments

The IFMOS detectors require an operating temperature of ≤ 30 K and the NIRCAM detectors can be somewhat above 30 K. All NIR instruments shall be passively cooled by the ISIM radiator system. The heat load budget shall not exceed 50 mW per NIR instrument.

The MIR detectors require temperatures between 8 K and 10 K, which requires active cooling.

	Arrays	Wires	8-10 K	~ 20 K	30 K ^{b)}	35 K	300 K ^{c)}
NIRCAM-FW 3 Filter Wheels ^{a)}	18	864 to FPU 78 to Instr.			25 mW	1.5 mW	27.2/18.2 W
NIRCAM-FTS 1 Filter Wheel ^{a)}	18	864 to FPU 76 to Instr.			25 mW	0.5 mW	27.2/18.2 W
IFMOS 1 Filter Wheel ^{a)}	10	480 to FPU 104 to Instr.			14 mW	0.5 mW	16.3/11.3 W
MIRCAM 2 Filter Wheels ^{a)}	2	90 to FPU 38 to Instr.	2.5 mW	0.5 mW		0.5 mW	2.5/1.9 W
MIRIFS 1 Filter Wheel ^{a)}	2	86 to FPU 34 to Instr.	1.5 mW	0.5 mW			1.7/1.3 W
Point. sensor FSM	4	192 to FPU 30 to Instr.				16 mW 100 mW	4.4 W
Total			4 mW	1 mW	64 mW	119 mW	

a) 50 mWs per step and wheel extrapolated from ISOPHOT, 36 steps per hour assumed

b) NIRCAM detectors can be above 30 K, mechanisms and electronics can be > 35 K

c) ADC Cont./Powersave

Table 2.3-1: Summary of instrument temperatures and dissipation

2.3.2 Thermal Design and Heat Load Budget of NIR Instruments

Each detector array of the NIR instruments is mounted separately onto the warmer instrument structure by means of a thermal decoupling device and is thermally connected to a thermal bus bar using a high purity aluminum or copper cooling strap, see Figure 2.3-2. The bus bar finally is attached to the ISIM radiator by a flexible cooling strap, too. To minimize parasitic irradiation from the warmer environment the cooling straps and the bus bar should have an emissivity of < 0.05 , e.g. goldized surfaces.

The parasitic heat from the instrument base plate to each detector array has been calculated assuming a thermal decoupling device with a thermal conductance of 0.32 mW/K. For a decoupling device made out of GFRP or Vespel this means a cross section to length ratio of about 1.8 mm. A principle design sketch of such a

configuration is outlined in Figure 2.3-2 as example. The effective cross section corresponds with, e.g. 20 mm diameter and 1 mm wall thickness. About the same conductance can be achieved using a tube with $\varnothing 18$ mm x 0.1 mm Ti alloy.

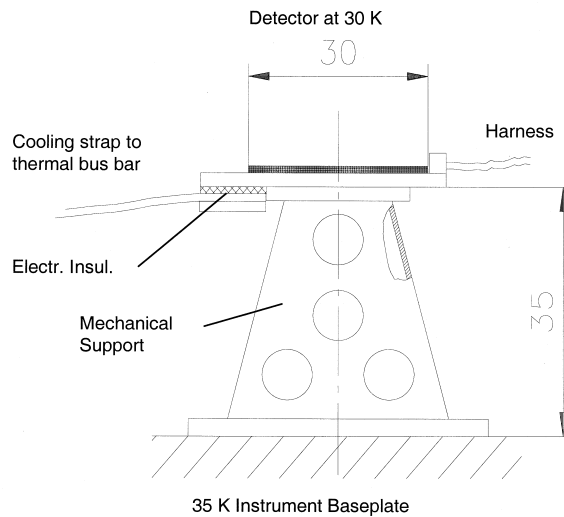


Figure 2.3-2: Detector thermal design principle

The detector cooling strap is made out of high purity aluminum or copper band with 1 mm x 30 mm cross section and a low emissivity surface (< 0.05). The length is assumed to 500 mm. The electrical insulation between cooling strap and detector can be provided with STYCAST adhesive, Diamond or Sapphire elements. Thus, in total a temperature gradient between detector and thermal bus bar in the order of only 0.1 K can be expected.

Based on the data listed in Table 2.3-1 and taking into account the above mentioned detector thermal design the following heat loads have been calculated for the NIR instruments:

	to 30 K heat sink		to 35 K instrument baseplate		Total heat load
	Detector Dissipation	Paras. Heat (struct+harn)	Filter Wheel Dissipation	Paras. Heat (harness)	
NIRCAM-FW	25 mW	6 mW ^{b)}	1.5 mW	2.5 mW	35 mW
NIRCAM-FTS	25 mW	6 mW ^{b)}	0.5 mW	2.5 mW	34 mW
IFMOS	14 mW	21 mW ^{a)}	0.5 mW	3 mW	39 mW

a) detector supports described in NGST/IFMOS Final Report. In addition, 4 mW parasitic heat onto cooling straps and thermal busbar are included

b) estimated

Table 2.3-2: NIR instrument dissipation and parasitic heat load

2.3.3 Passive Cooling Concept for NIR Instruments

The NIR instruments power dissipation together with additional dissipation from other components inside the ISIM need to be rejected by radiative cooling. Black or white painted open honeycomb with 0.9 emissivity is proposed as radiator surface. Figure 2.3-3 shows the radiator temperature versus the radiator size for different heat loads rejected by such a radiator. The curves in this figure are calculated using the Stefan-Boltzmann's law and an estimated view factor to space of 82%. Further, an efficiency of the radiator area of 97% has been considered, which has been calculated for a 2 mm aluminum (Al 7075) face sheet and a radiator temperature of 30 K.

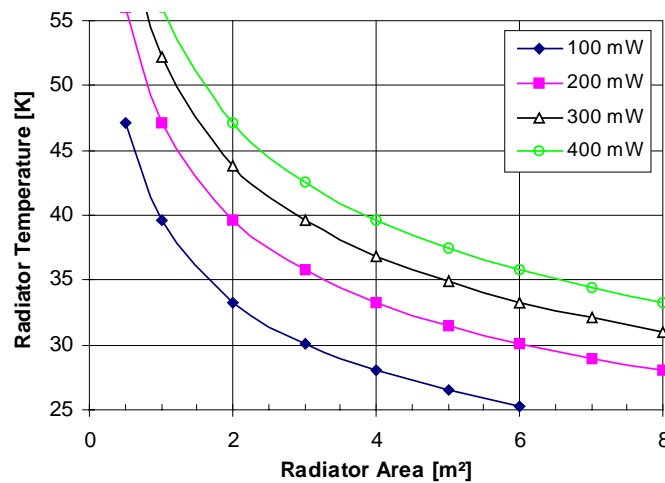


Figure 2.3-3: Radiator temperature versus radiator size for different heat loads [emissivity: 0.9; view factor: 0.82; efficiency: 0.97 (2 mm Al 7075 at 30 K)]

The heat load shown in Figure 2.3-3 consists however of the instrument power dissipation and the parasitic heat flow into the ISIM and/or to the radiator. This parasitic heat load has been calculated by means of a Thermal Mathematical Model (TMM) assuming the IR emissivities of the geometric surfaces as indicated in Figure 2.3-1. The radiator temperature has been calculated for different instrument power dissipation rates assuming the maximum ISIM radiator area of 8.25 m². The results are shown in Figure 2.3-4. In this case the total radiator heat rejection capability at 30 K is about 320 mW and the parasitic heat load share into the ISIM is nearly 100 mW. Thus, about 220 mW remains for the instruments power dissipation at a radiator temperature of 30 K. Considering further a margin of 30%, the total instrument power dissipation at 30 K is limited to 170 mW.

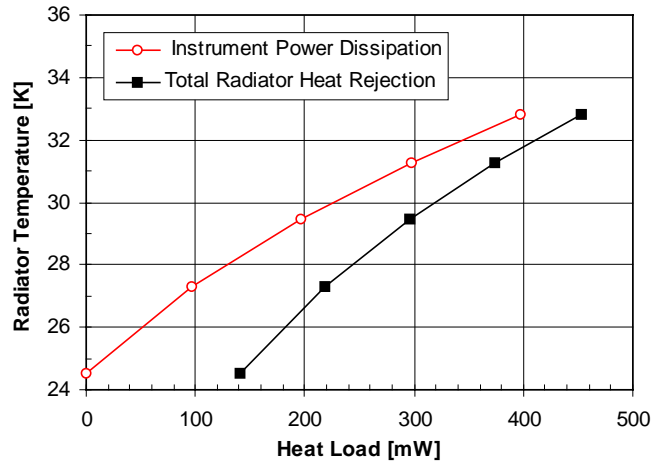


Figure 2.3-4: Maximum cooling capacity of an ISIM radiator with 8.25 m² area [TMM calculation; efficiency: 0.97]

2.3.4 Thermal Design and Heat Load Budget of MIR Instruments

MIRCAM Thermal Design

The MIRCAM (LW) principle thermal concept is shown in Figure 2.3-5 together with the temperature requirements of the optical components. For the long wavelength path the movable filter wheel need to be cooled to 22 K. Therefore, the filter wheel is mounted into a thermally insulated box made of aluminum, which itself is actively cooled to about 18 K using a high purity aluminum cooling strap. Thus, the wheel cooling is provided by the 18 K box. Other cooling methods, such as cooling across the wheel bearings only or by means of a sapphire tip pressed onto the wheel shaft were investigated and tested during the ISOPHOT project and found as inadequate.

The thermal insulation of the 18 K box is provided by six thin-walled CFRP struts with 20 mm diameter, 2 mm wall thickness and 400 mm length, see Figure 2.3-6. To minimize radiative heat exchange the external surface of the box should have a low emissivity of ≤ 0.05 (goldized). Due to straylight reasons the internal surface need to be black (emissivity >0.90). As determined from the corresponding drawing file, the (goldized) external surface is about 0.36 m² and the area of the apertures is 0.025 m².

The long wavelength detector array is mounted inside the 18 K box, too. As support structure a thin-walled titanium alloy tube with (18 x 0.1) mm diameter and 30 mm length is proposed. To cool the detector to 10 K, a second cooling strap is connected to an active cooling system. Therefore, a thermally and electrically insulated, but light-tight feed-through is necessary.

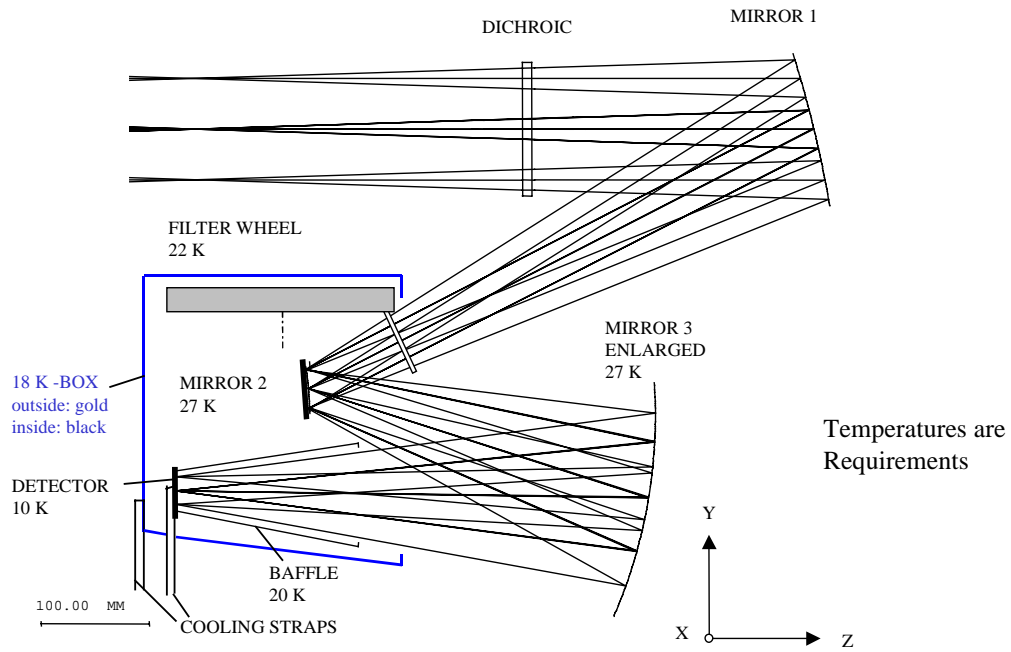


Figure 2.3-5: MIRCAM-LW thermal design principle and temperature requirements

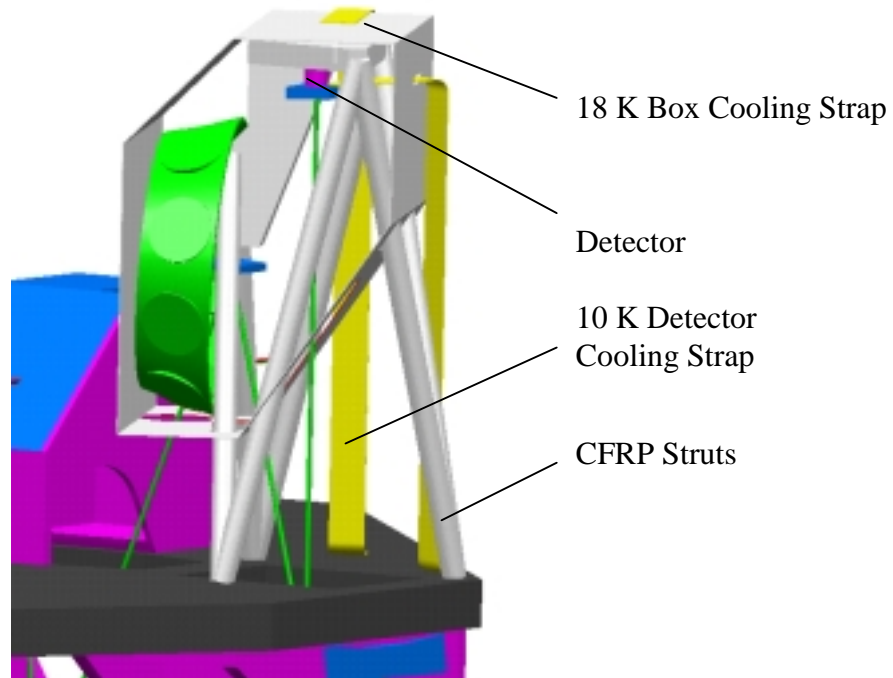


Figure 2.3-6: Thermal design of MIRCAM-LW, side walls of 18 K box not shown

For the short wavelength path no filter wheel cooling is required. The short wavelength detector array is therefore mounted directly onto the warmer instrument structure by means of the same thermal decoupling device and also thermally connected to the active cooling system using a high purity aluminum cooling strap.

MIRIFS Thermal Design

For the long wavelength path the MIRIFS thermal design concept is shown in Figure 2.3-7. The filter wheel, mirror 6, mirror 7 and the detector is enclosed in a 18 K box as described in the previous section. The thermal insulation of the 18 K box is provided by six thin-walled CFRP struts with 20 mm diameter, 1 mm wall thickness and 150 mm length. The (goldized) external surface of this box is about 0.33 m² and the aperture area is 0.0074 m². The detector is decoupled from the box by the same support structure as used for the MIRCAM and connected to the active cooling system using an aluminum cooling strap with a feed-through through the 18 K box wall.

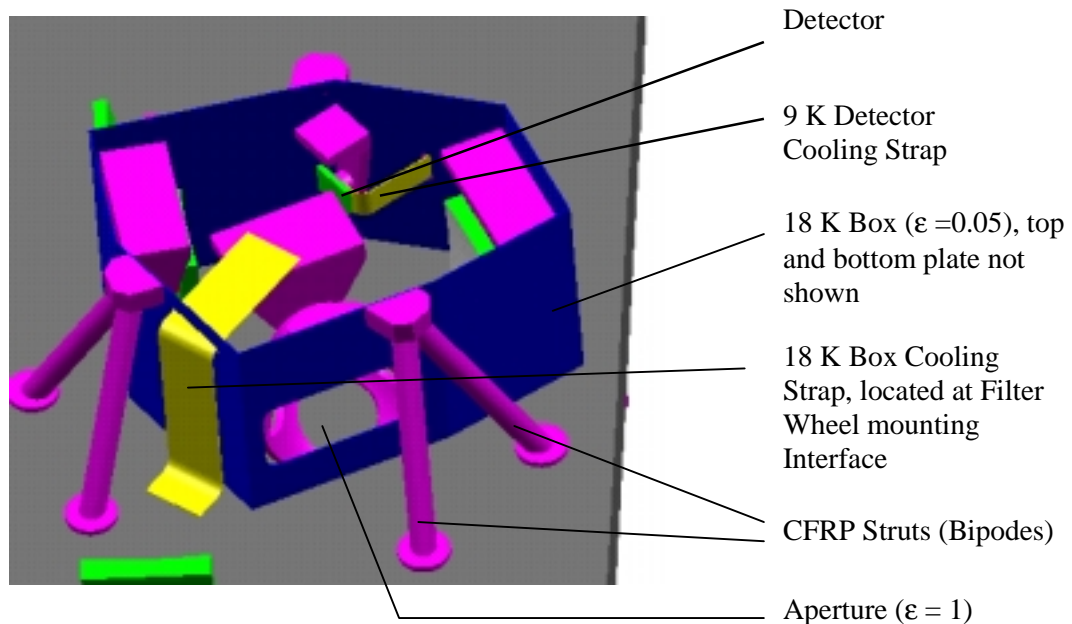


Figure 2.3-7: Thermal design of MIRIFS-LW

The thermal design of short wavelength path is shown in Figure 2.3-8. In this case only the mirror 7 and the detector is enclosed in a 18 K box. The thermal insulation of the 18 K box is also provided by six thin-walled CFRP struts with 20 mm diameter, 1 mm wall thickness and 150 mm length. The (goldized) external surface of the short wavelength box is about 0.44 m² and the aperture area is 0.0091 m². The detector thermal design is the same as for the long wavelength path.

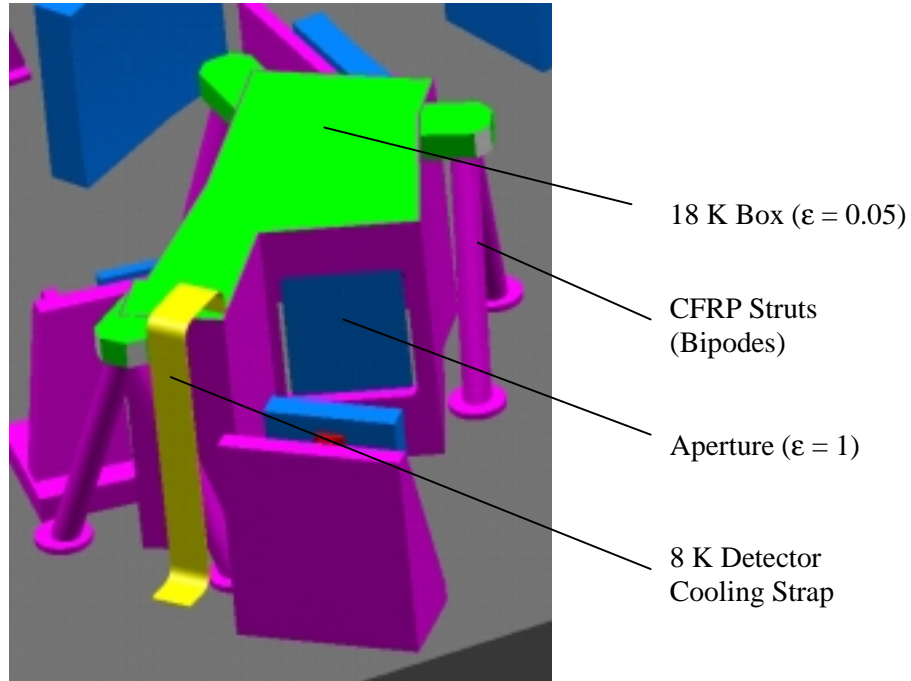


Figure 2.3-8: Thermal Design of MIRIFS SW

Heat Load Budget of MIR Instruments

Based on the previously described design and taking into account the data listed in Table 2.3-1 the parasitic heat loads have been calculated for the relevant instrument components. For the calculations a 40 K radiative environment is assumed. Concerning the harness 2 m long stainless steel wires thermalized at 100 K are assumed. As wire diameter 0.5 mm for mechanisms and 0.1 mm for the FPU components and sensors are taken.

The heat flow chart for the MIR instruments is presented in Figure 2.3-9 and the total cooling demand required for the MIR instruments is as follows:

Total Cooling Demand of MIR instruments at 8 K:	15 mW (18 mW)*
Total Cooling Demand of MIR instruments at 18 K:	26 mW (34 mW)*
Total Cooling Demand of MIR instruments at 30/35 K:	3 mW

*) assuming 35 K instrument baseplate temperature

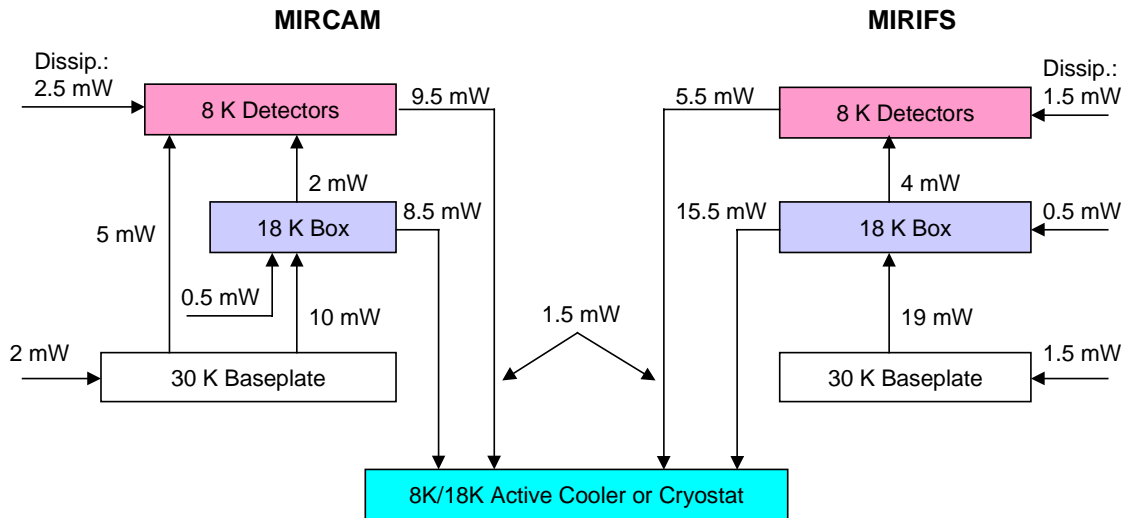


Figure 2.3-9: Heat flow chart of MIR instruments

2.3.5 Cooling Concepts for MIR Instruments

Technical Cooling Solutions for 2 - 20 K

The various types of cooling methods to be considered in the trade-off can be subdivided into following basic categories:

Cryogen Storage:	Liquid Helium	IRAS, COBE, ISO, (FIRST)
	Solid Hydrogen	SPIRIT III
	Solid Neon	CLAES
Mechanical Cooler:	Joule-Thomson	(FIRST, PLANCK)
	Brayton Cycle	
	Pulse Tube	
Sorption Cooler:	Hydrogen	BETSCE, (PLANCK)
Hybrid Systems:	Joule-Thomson cooler with radiant pre-cooler	
	Cryogen storage with mechanical pre-cooler, etc.	

Cryogen Storage Coolers

Figure 2.3-10 shows the specific enthalpy of cryogenic coolants versus cooling temperature.

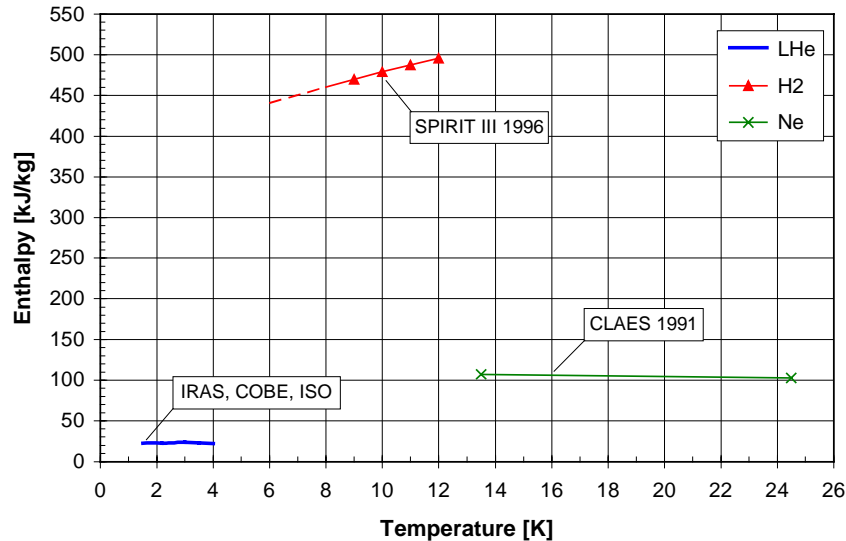


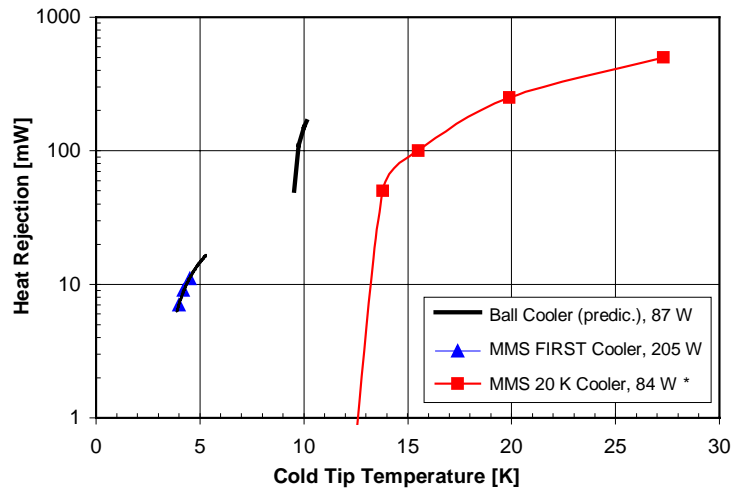
Figure 2.3-10: Specific cooling capacity of cryogen coolants between 2 K and 20 K

Solid Hydrogen possesses a very high specific enthalpy compared to the other ones. For a 10 years lifetime the required amount of coolant per cooling power can be calculated to

- 0.7 kg H₂ /mW (8.1 ltr. H₂ /mW) for solid hydrogen
- 3.0 kg Ne /mW (2.1 ltr. Ne /mW) for solid neon
- 13.7 kg LHe /mW (93.9 ltr. LHe /mW) for liquid helium

A liquid helium cryostat is not suitable, since it requires a too high mass and volume. For a heat load of 30 mW for example the LHe mass would be more than 400 kg and the corresponding volume more than 2800 l, which is more than the amount foreseen for FIRST. A solid neon cooler is not suitable for temperatures lower than 13 K, it may be suitable as a second stage for a solid hydrogen cooler. Thus, the solid hydrogen cooler therefore remains as the most promising coolant out of the cryogen storage coolers. This cooling concept therefore is investigated in more detail in the following section.

Figure 2.3-11 shows the heat rejection capability of some promising coolers versus cooling temperature. For the MMS coolers ground test data are available and the qualification of the MMS 4 K (FIRST) cooler will be completed in 1999. For the Ball cooler and other cooler types (e.g. Sorption or Brayton cooler) currently only performance predictions are available.



* * power of electronics not included

Figure 2.3-11: Heat rejection capability of mechanical coolers below 30 K

The integration of a mechanical cooler onto the ISIM has to be such, that exported vibration and parasitic heat load from the cooler is minimized. Thus, concerning for example the MMS/RAL 4 K cooler, the compressors should be located as far away as possible from the detectors. The Stirling cycle pre-cooler is used to pre-cool the 4 K system, so the first two stages of cooling are at 160 K and at 20 K. The 4 K stage can be situated remotely from the pre-cooler provided that it is in the correct thermal environment. The length of this heat exchanger is about 1.3 m. The distance from the tip of the pre-cooler and the 4 K stage can therefore be up to this distance.

The Stirling cycle pre-cooler however needs to be located close to its compressors and for these items there is a maximum separation of 0.5 m. Thus, the Stirling pre-cooler has to be well insulated and the power dissipation (84 W) has to be transferred by means of a heat pipe or capillary pumped loop to a hot radiator (300 K) located at the NGST service module. The JT (4 K) system compressors on the other hand can be remote from the pre-cooler and there can be quite long tubes used to connect to the cold plumbing.

Envelope, Mass and Power Consumption of the MMS FIRST- 4 K Cooler:

Stirling Compr. Unit:	Ø 120mm x 238mm, 14 kg	64 W (80 W max)
JT Compressor Unit:	Ø 120mm x 238mm, 14 kg	60 W (100 W max)
Displacer/4 K Stage:	Ø 78mm x 220mm, 0.25 kg	20 W (26 W max)
Ancillary Equipment::	6 kg	9 W (15 W max)
Electronics:	TBD	52 W

Solid Hydrogen Cooler Concept

To determine the performance of a solid hydrogen cooler on ground and in orbit, a simplified thermal mathematical model describing the couplings between cryostat vacuum vessel, thermal shields and tank has been established. A principal sketch is given in Figure 2.3-12 showing the vapor cooled shields and the shrink fit coupling which connects the detector cooling straps to the solid hydrogen tank after cool down in orbit. The tank and the thermal shields are covered with MLI. As baseline the cryostat has been preliminary designed for a net heat load of 43 mW at 8 K operating temperature for 10 years lifetime.

The thermal analysis for the preliminary design revealed the following results:

Amount of Solid Hydrogen:	40 kg (460 l)
Total mass of cryostat:	~ 140 kg
Total envelope of cryostat:	Ø1.1 m x 1.4 m
Parasitic heat into hydrogen tank:	8 mW in orbit (40K) 2.1 W on ground (300 K)
Net cooling power at 8 K:	43 mW

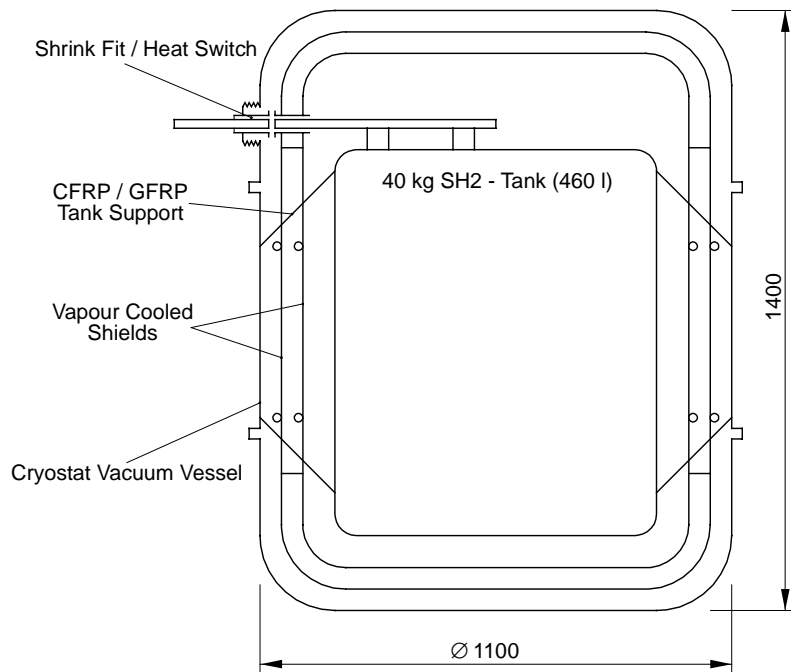


Figure 2.3-12: Principle design of a solid hydrogen cooler

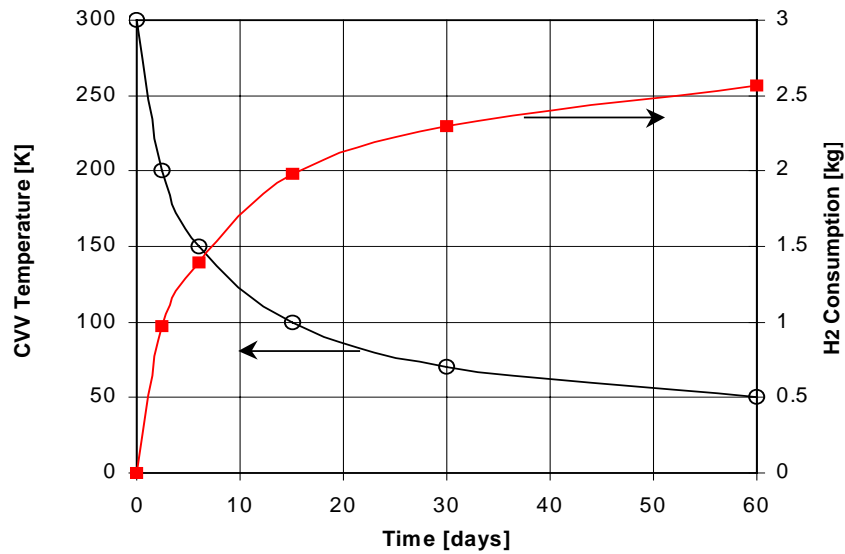


Figure 2.3-13: Solid hydrogen consumption during orbital transient phase

The thermal analysis results revealed further, that even without instrument heat load the temperature of shield 1 is larger than 25 K. Therefore also the instrument heat load at 18 K level has to be added directly to the tank. Due to the low environment temperature of maximum 50 K the instrument heat load is the dominant heat load on the tank. The solid hydrogen consumption during the orbital transient phase is less than 3 kg assuming a cool-down phase of 60 days, see Figure 2.3-13. For an instrument heat load of 30 mW the lifetime is calculated to 10.3 years. For a heat load of 40 mW the lifetime will be reduced to 8.4 years. The thermal analysis results are summarized in following Table 2.3-3.

	Orbital Equilibrium		Ground Equilibrium
	for $Q_{instr} = 30 \text{ mW}$ at 10 K	for $Q_{instr} = 40 \text{ mW}$ at 10 K	
Tank	~ 10 K	~ 10 K	~ 10 K
Shield 1	28.7 K	26.9 K	158 K
Shield 2	40.0 K	38.9 K	245 K
Cryostat Vessel	50K	50 K	300 K
Mass Flow	0.083 mg/s $\cong 10.3 \text{ yrs. operat. lifetime}$	0.102 mg/s $\cong 8.4 \text{ yrs. operat. lifetime}$	4.5 mg/s
Parasitic Heat into SH ₂ Tank	10 mW	9 mW	2.1 W

Table 2.3-3: Analysis results for the preliminary solid hydrogen cryostat design [the data in this table are based on 50 K environment]

The mass flow during ground operations and launch preparation can be minimized by auxiliary LHe cooling of the tank and the shields. The launch autonomy without access of 1-2 days can be elongated by sub-cooling the tank and the shields with LHe.

During phase 2 it turned out, that the operating temperature of some MIR detectors need to be reduced to about 8 K. This requires about 4% higher mass of hydrogen with respect to 10 K tank temperature (see Figure 2.3-14) and a pressure drop across the vent line system of 0.1 mbar, see Figure 2.3-15. Since also 0.1 mbar pressure drop has been extrapolated from the ISO ventline with 0.1 mg/s hydrogen at 40 K, an operating temperature of 8 K solid hydrogen is considered feasible using a proper ventline design.

A summary of Solid Hydrogen cryostat design data for various performance assumptions is provided in Table 2.3-4.

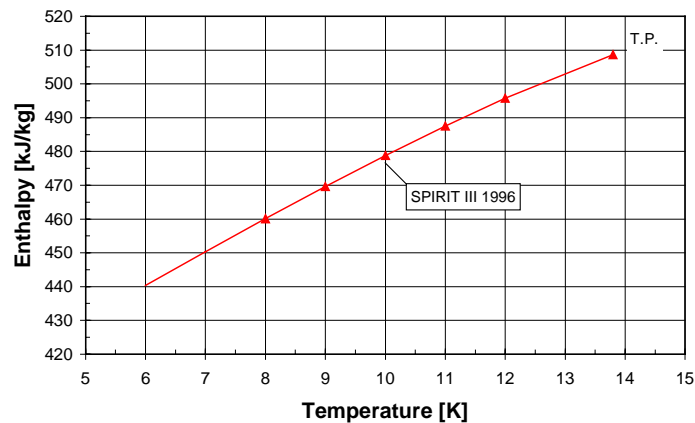


Figure 2.3-14: Solid hydrogen specific enthalpy versus temperature

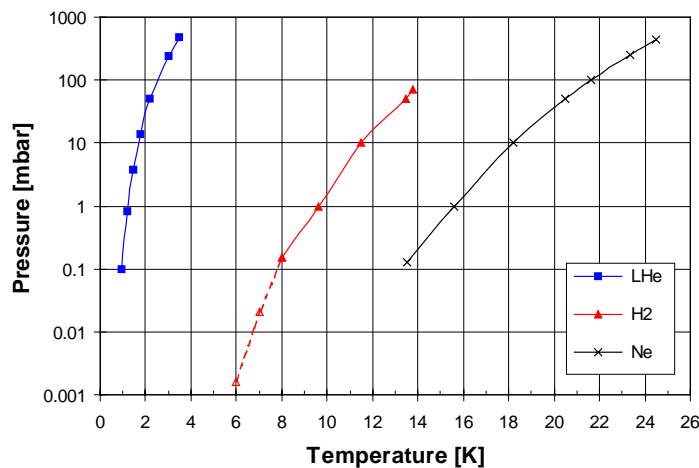


Figure 2.3-15: Vapor pressure of different coolants versus temperature

Coolant	Temp	Heat Load	Parasitic Heat Load	Mass	Envelope	Lifetime
30 kg (350 l) SH ₂	10 K	40 mW	9 mW ^a	140 kg	Ø1 x 1.35 m	8.4 yrs.
30 kg (350 l) SH ₂	10 K	30 mW	10 mW ^a	140 kg	Ø1 x 1.35 m	10.3 yrs
30 kg (350 l) SH ₂	8 K	42 mW	7 mW ^b	140 kg	Ø1 x 1.35 m	8.2 yrs.
40 kg (460 l) SH ₂	8 K	43 mW	8 mW ^b	175 kg	Ø1.1 x 1.4 m	10 yrs.

a) 50 K environment assumed (older calculations)

b) 40 K environment assumed

Table 2.3-4: Solid hydrogen cryostat design options

Summary and Conclusions

The performance data of the different active cooling concepts for the MIR instruments are compiled in Table 2.3-5.

Concept	Temp.	Heat Load	Mass at ISIM	Power	Status
Solid Hydrogen 30 kg (350 l) 40 kg (460 l)	10 K 8 K	30 mW ^d 43 mW	140 kg 175 kg	0	technology applied in space
JT stage & Sorption	8 K & 20 K	10 mW & 110 mW ^a	35 kg ^b	80 W & 50 W ^c	sorption principle demonstrated
Brayton Cooler	6 - 8 K	20 -180 mW	40 kg ^c	100 W	65 K cooler flown on STS-95

a) scaled down from PLANCK

b) plus 40kg compressor, plus tbd for radiator

c) radiator for pre-cooling at ~ 50 K / 220 K to be added

d) for 50 K environment (baseline assumption is 40 K)

Table 2.3-5: Cooling concepts for the long wavelength MIR instruments at 6-10 K

The solid hydrogen storage is a promising concept because there are no movable parts. It therefore possesses a high reliability and the technology has been already applied in space. A drawback is the high mass and envelope at ISIM. Other promising concepts currently developed are a Brayton cooler (Creare) for NGST cooling demand and a 4 K Joule Thomson cooler (MMS) with a 20 K Sorption Precooler (JPL) for PLANCK. These concepts however require additional radiators at or near the ISIM.

Because of the high impact on system level design and budgets the final cooler selection is considered a system level task.

2.4 Detectors

The NGST instruments require detectors which shall cover a wide spectral range from the visible to the mid-infrared, respectively from 0.6 μm to 28 μm . In table 4.3.1 detector requirements for the various studied instruments are listed.

Instrument	Range	Detector Size	Pixel Size	Dark Current	Top
	μm		μm	e-/sec	K
VIS/NIR FW	0.6 - 5	12K x 6K	18.5	< 0.02	< 35
VIS/NIR FTS	0.6 - 5	12K x 6K	18.5	< 0.1	35
IFMOS, LR	1 - 5	6 x 2K x 2K	18.5	< 0.02	< 35
IFMOS, HR	1 - 5	4K x 4K	18.5	< 0.002	< 30
MIRCAM SW	5 - 10	2K x 2K	27	< 1	< 9
MIRCAM LW	10 - 28	1K x 1K	27	< 10	< 10
MIRIFS SW	5 - 10	2K x 1K	27	< 0.1	< 8
MIRIFS LW	10 - 28	1K x 1K	27	< 1	< 9

Table 2.4-1: Detector requirements for NGST instrumentation

2.4.1 Near Infrared (NIR) Detectors

For NGST applications these detectors have to fulfil very demanding requirements:

- very low dark noise
- very low read noise
- very low power dissipation
- very large size of detector array

The most promising detector materials for the NIR spectral range are InSb and HgCdTe.

InSb-Detector Arrays

InSb detector arrays cover the total spectral range from 1 to 5 μm with fairly high quantum efficiency (Q.E) of 85 % - 90%, see Figure 2.4-1. The largest manufactured InSb array is the ALADIN 1024x1024 array with 27 μm pixel size. This array is designed and manufactured by Raytheon (SBRC) for ground based astronomic observations. For this application the multiplexer is divided in 4 fully independent quadrants with 1-8 selectable readouts each. InSb detector arrays with 256x256 and 512x412 elements have been manufactured and thoroughly tested for space programs like SIRTf and IRIS respectively.

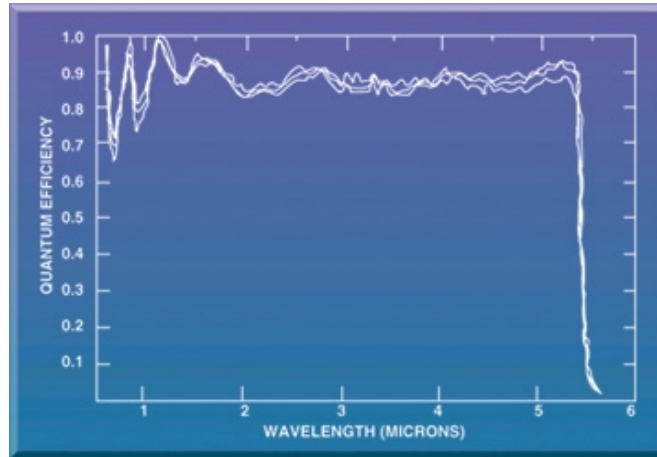


Figure 2.4-1: InSb spectral response

- Dark Current

At the time being Raytheon demonstrated mean dark current measurements of < 0.02 e-/sec @ 35K for one output of a 256x256 array. ESO even achieved 0.004 e-/sec @ 25K evaluating a subsample of the 1Kx1K ALADIN array at reasonable reversed bias setting. These results show clearly that the demanding dark current requirements in particular for the spectrograph (IFMOS) are achievable with InSb detector arrays. However these data have to be verified for an entire 1Kx1K or even 2Kx2K array. Raytheon is optimistic to achieve this goal.

- Readout Noise

The readout noise is generated by the multiplexer and mainly dependent on the cell unit and line driver design. In general, read noise figures are in the order of 50 - 80 e-rms for single readout. Improvements have been demonstrated applying CDS, Fowler sampling or ramping-up techniques. For multiple readout the noise figures are in the order of 10 - 20 e-rms dependent on the number of Fowler sampling pairs and samples during ramping-up. Raytheon achieved 6 e-rms with 32 Fowler sampling pairs. In the framework of NGST a new MUX is in development to improve the readout noise with the aim to achieve 15 e-rms for single readout.

- Multiplexer

The a.m. new, dedicated 1Kx1K cryo-CMOS-MUX with 27 μ m pitch provides a reference circuit to compensate electronic and thermal drifts. For test purposes 4 outputs are implemented, however, only 1 output per 1Kx1K array is foreseen for the flight units. The design is such that all bond pads are on one side. This allows a 3 sided butttable focal plane layout. This MUX is planned to be used for the 1Kx1K Si:As arrays as well. As a back-up solution Ball Aerospace subcontracted to Raytheon a 2Kx2K multiplexer design. The first 1Kx1K Cryo-MUX sample shall be available middle of this year, according to Raytheon.

InSb detectors can be used to sense down to 0.6 μm , see Figure 2.4-1. The wiggles come from the appropriate coating. An extension of the IFMOS to the visible range based on InSb detector arrays might be an valuable option.

Currently InSb detectors are the largest and most suitable detector arrays for IFMOS as concerns dark current, readout noise and maturity.

HgCdTe-Detector Arrays

Photo-voltaic HgCdTe detectors cover a wide spectral range from 1 μm to approx. 17 μm , depending on the composition of their constituents. In the range from 1 to 2.5 μm optimized 1Kx1K HgCdTe detector arrays with 18.5 μm pixel pitch are available from Rockwell. The average quantum efficiency is about 60% and drops to 50% at about 0.8 μm . This HAWAII-1 array is manufactured for ground based astronomic applications and shows very good performance data at convenient operating temperatures of about 70 K. In order to cover the total NIR range from 1 to 5 μm Rockwell grows new HgCdTe /CdZnTe materials with different techniques. Rockwell gained space flight experience with the manufacture of 256x256 HgCdTe detector arrays with 40 μm pitch and 2.5 μm cut-off for the NICMOS camera on the Hubble telescope.

- Dark Current

Dark noise values for the HAWAII-1 with 2.5 μm cut-off have been measured down to < 0.01 e-/sec @ 43 K. First samples of a 256 x 256 HgCdTe /CdZnTe array with 5.2 μm cut-off show dark currents of < 0.4 e-/sec @ 50 K. The latest dark noise data were retrieved from a 1Kx1K array with 5.2 μm cut-off which has been manufactured and delivered to University of Hawaii for test purposes. This array consists of four 512x512 HgCdTe detectors bonded to a 1Kx1K HAWAI-1 multiplexer. Preliminary test data indicate dark current values of 0.08 e-/sec @ 67 K. Further investigations and tests are ongoing.

- Read Noise

The read noise of the HAWAII-1 MUX has been measured down to 3 e- rms with 64 Fowler sample pairs (ESO), which meets the NGST requirement. Read noise data of the new developed HAWAII-2 MUX are not known yet.

- Multiplexer

Rockwell developed and manufactured a new 2Kx2K, 18 μm pixel pitch (HAWAII-2) mutliplexer for groundbased astronomic application. New features and improvements, such as reference circuit and an improved unitcell as well as line driver design to reduce glow are implemented. Due to the latter effect, the HAWAII-1 arrays are usually operated with an external line driver, which adds additional heat load. The new 2Kx2K array consists of four quadrants with 8 signal and 1 reference signal output each. Bond pads are on four sides. Data about the amount of glow

reduction and reference circuit capability are not published or tested yet. A dedicated MUX design for NGST is not known yet.

With appropriate treatment such as thinning HgCdTe detectors might be sensitive down to 0.6 μm and might be an option for NIRCAM as well.

In general HgCdTe material offers a lot of various possibilities. However, developments in material growing techniques and improvements of current detector technologies are still ongoing to suit the NGST requirements.

Two major projects important for NGST are conducted at the Rockwell Sciences Center:

- Growing and testing of suitable HgCdTe/HgZnTe material for 5 μm cut-off detectors
- Development and manufacturing of 2Kx2K arrays (HAWAII-2) with 2.5 μm cut-off

Rockwell is focusing on the HAWAII-2 developments and plans to deliver the first 2Kx2K HgCdTe arrays with 2.5 μm cut-off to ESO in October 1999, produced on best effort basis.

Detector Array Configurations

2Kx2K focal plane arrays with 5 μm cut-off are not yet available but are in development at Raytheon and Rockwell. Rockwell focuses their developments on single large 2Kx2K arrays, while Raytheon prefers to build 1Kx1K arrays. Raytheon's approach is mainly driven by the yield aspect. As a back-up solution Ball/Raytheon are designing a 2Kx2K multiplexer. As a simple approach, 2Kx2K focal plane arrays can be built by butting four 1Kx1K arrays on a common motherboard. For the spectrographic application, of course, no gaps in between would be preferable.

Figure 2.4-2 depicts an example of 2Kx2K and Figure 2.4-3 examples of 4Kx4K array assembly configurations. Based on buttable Raytheon 1Kx1K arrays the gap sizes are < 0.75 mm and < 1.5 mm respectively for a 2Kx2K configuration. The maximum gap size of < 5 mm appears for a 4Kx4K configuration. The calculated filling factor for such a 2Kx2K array is in the order of 99%, for a 4Kx4K array it drops to about 92%. In order to minimize spectral loss the maximum gap sizes shall be along the geometrical resolution. The 4Kx4K configuration can be built out of four 2Kx2K arrays, if available. This reduces the number of gaps significantly. At the time being Rockwell 2Kx2K MUX design has bond pads on four sides and does not foresee any butting capabilities. Taking 5 mm gap size for the Rockwell approach into account the filling factor is about 88%.

The array configurations are preliminary and may change during phase A & B. Raytheon proposed additional configurations on the detector workshop in Baltimore.

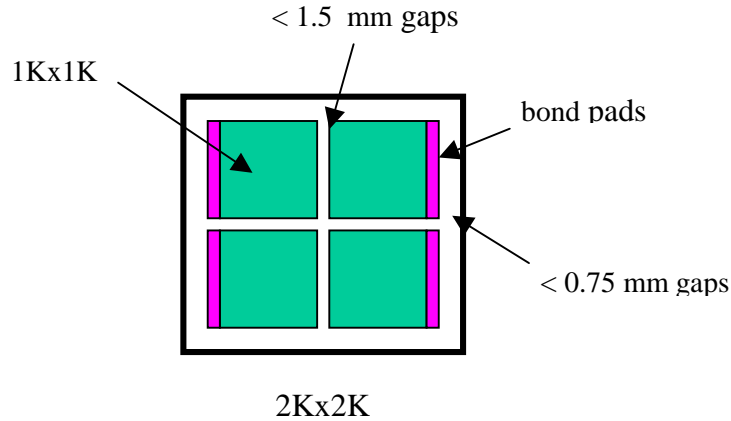


Figure 2.4-2: Possible array configuration for an assembled 2Kx2K detector array (Raytheon).

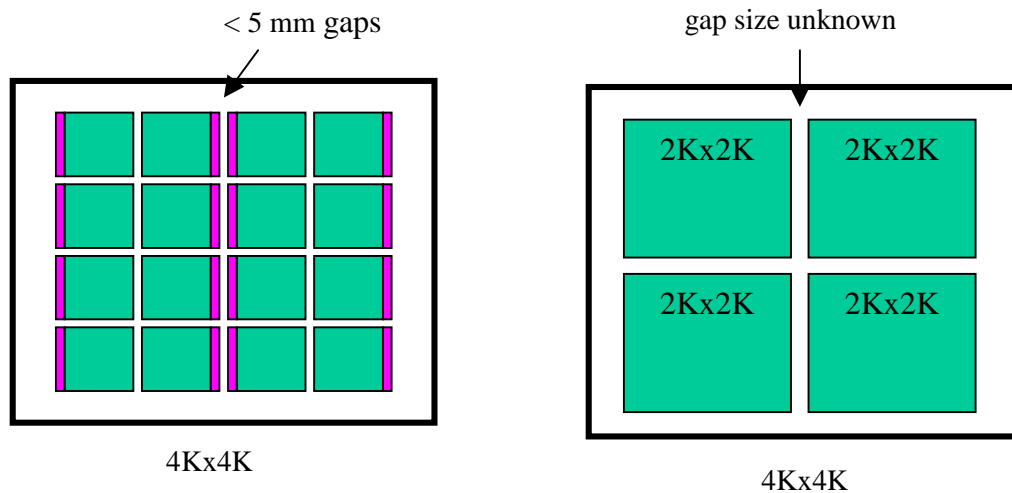


Figure 2.4-3: Sketches of 4Kx4K array configurations. Left: Raytheon approach; Right: Rockwell approach. (Not scaled!)

2.4.2 Mid Infrared Detectors

The medium infrared region covers the spectral range from 5 μm to 28 μm . The instrument requirements are not such demanding, see Table 2.4-1, but

- low dark noise
- low readout noise
- very low power dissipation
- large size of detector array

are requested as well.

The 5 to 28 μm region is split up into two bands 5 to 10 μm and 10 to 28 μm mainly due to background radiation. This supports the development of HgCdTe detectors with 10 μm cutoff which shall operate at nominal ISIM temperature of approx. 30 K. It would allow to operate MIR instruments with 10 μm cut-off without any additional cooling devices.

- **HgCdTe Detectors Arrays with 10 μm cut-off**

NASA subcontracted to Rockwell/University of Rochester the development of 10 μm cut-off HgCdTe detector arrays with the aim of 100 e-/sec dark current @ 30K. Tests revealed much higher dark currents in the order of 1000 e-/sec @30K for single detector elements. The dark current seems to be limited by G-R and tunneling currents. For improvement further material studies and processes have to be performed and investigated. As a conclusion, large detector arrays with fairly low dark currents (<1 e-/sec) will be not available for NGST. The technology is regarded as too pre-mature.

- **Si:Ga IBC Detector Arrays**

Gallium doped silicon impurity band conductor arrays are sensitive up to 18 μm and operate at low temperatures. Si:Ga IBC detectors are selected as a back-up solution for Si:As IBC due to higher operating temperature of about 3-4 K, 10 –14 K respectively, and expected similar low dark current (1-10 e-/sec). The use of Si:Ga IBCs would relax the cooling constraints for the MIR instruments by far. Thus NASA subcontracted to Boeing the development of large Si:Ga IBC arrays for NGST. At the time being Boeing is still in the process to grow the best suited material. Measurements are performed on comparable large test samples which indicate that the dark current requirements might be achievable in future.

- **Si:AS IBC Detector Arrays**

The most promising and mature detector arrays for the mid-infrared region with 28 μm cut-off are Si:As detectors from Raytheon. These 256x256 arrays have been manufactured and thoroughly tested for the IRAC instrument on SIRTf. With respect to the NGST requirements Si:As IBC show very good performance, however with the penalty of very low operating temperature in the range from 6 to 10 K. The Q.E is 40% to 50% and it drops down to 10 % at 28 μm , compare Figure 2.4-4.

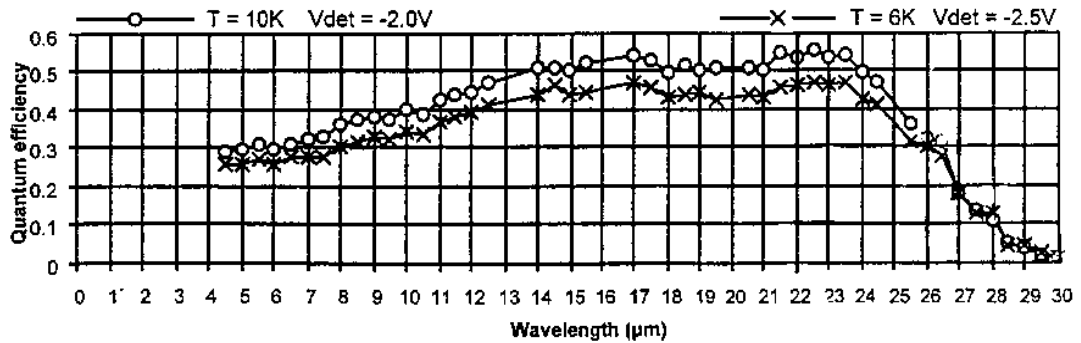


Figure 2.4-4: Quantum efficiency vs. wavelength at 6 K and 10 K of Si:As (ref. SPIE Vol. 2816/165)

- Dark Current

Dark currents have been measured to < 1 e-/sec @ 8K and even down to < 0.4 e-/s @ 6K with SIRTf arrays. Figure 2.4-5 shows the dark current as a function of temperature, extrapolated to very low dark currents. Deviation in the later regime may occur. Dark current requirements for the MIRCAM and MIRIFS, LW with < 1 e-/s are achievable, however, dark current requirements for the MIRIFS with < 0.1 e-/s seem to be difficult. Raytheon is going to investigate dark current limitations in order to improve these noise figures for the Si:As arrays.

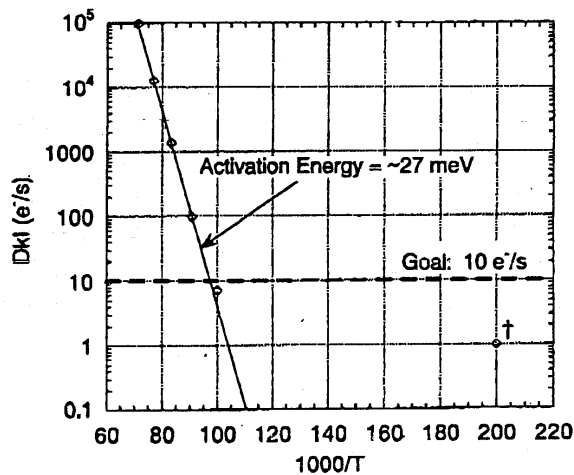


Figure 2.4-5: Dark current vs. temperature (Ref.: "Si:As IBC Focal Plane Arrays", A.D. Estrada et.al., SPIE Vol 3354, 3/98)

- Readout Noise

Readout noise figures will be comparable to those for the InSb array, because Raytheon foresees to use the same Cryo-MUX (1KX1K) for InSb and Si:As in the NGST project. Readout noise of < 15 e- rms with 16 Fowler sample pairs @ 6K (for IRAC < 20 e- rms @ 6K) has been measured with the 256x256 IBC arrays. Improvements are ongoing at Raytheon to achieve better readout noise figures.

- Detector Array Configuration

The maximum array size for the MIR instruments will be 2K x 2K for the camera and 1K x 2K for the spectrograph. This can be easily achieved using the Raytheon 3 sided buttable cryo- multiplexer. The gaps between the arrays will be < 0.75 mm and < 1.5 mm respectively, compare also IFMOS configurations.

As a conclusion the current Si:As performance data meet already the MIR instrument requirements with the exception of MIRIFS SW instrument due to the very low dark current requirement. The Si:As arrays have been tested thoroughly for SIRTf and are regarded as mature.

The manufacture of a 1K x 1K Si:As IBC with 27 pixel size is expected as not critical, and it is planned for year 2001.

2.4.3 Detector Performance Summary

Based on current investigations InSb and Si:As detector arrays have very good potential for NGST and even meet already some of the listed requirements, see performance summary Table 2.4-2. The new Cryo-MUX development aims for 15 e- rms single readout. Depending on the readout scheme and number of sample pairs (NS) the readout noise requirements might be met, in particular for Si:As arrays. Dark current requirements of 0.1 e-/sec for the MIRIFS SW seem to be difficult to achievable.

Ongoing developments and tests wrt. the 1K x 1K HgCdTe with 5 μ m cut-off arrays are very promising. The availability of 2K x 2K arrays with 2.5 μ m cut-off is planned for fall this year 1999.

Detector	Wave-length	Detector Size	Pixel Size	Dark Current	Readout Noise	T _{op}	Heat Dissip.
	μm		μm	e-/sec	e- rms	K	mW
InSb	1 - 5	1K x 1K 2K x 2K ³⁾	27	< 0.02	< 6, NS=36	35	< 1 < 2 - 4
HgCdTe	1 - 2,5	1K x 1K 2K x 2K ¹⁾	18 18	< 0.01 tbd.	< 5 tbd.	43	< 1 < 2 - 4
HgCdTe/ HgZnTe	1 - 5 5 - 10μm ³⁾	1K x 1K ²⁾ 2K x 2K ²⁾ single element	18 40	< 0.08 < 10x4	5 - 10 tbd..	67 30	< 2 - 4 tbd.
Si:As		256 x 256 1K x 1K ³⁾	30 27	< 0.4 (< 0.4)	15-20, NS=16 (5 - 10)	6 tbd.	0.5 < 1

1) manufactured at Rockwell

2) under development for 1 - 5 μm

3) under development at Raytheon

Table 2.4-2: Detector performance summary

It should be noted that the detector selection will not only be based on the above mentioned performance requirements. There are much more criteria which have to be considered and defined at least before begin of Phase A. As an example, the detector yield is an important issue, because it drives schedule and cost. Latent images, glow, pixel size, number of leads and operability might be e.g. further criteria. In addition a final selection can only be performed having a detailed test procedure and well defined test conditions and environment.

As a conclusion it can be stated that the current detector availability and developments are very promising to suit the NGST requirements.

2.5 Electrical Design

2.5.1 Instrument Electrical System Overview

The tasks of the instrument electrical system include the acquisition of images with a detector, conversion into analog and digital representation by a signal processing chain, on-board image processing and storage for transmission by the spacecraft to ground.

The electrical system components are distributed at various locations on the spacecraft, depending on their functionality and with respect to overall spacecraft requirements. A major constraint is the minimization of heat dissipation inside ISIM. Only essential electrical components are located there. Signal processing electronics is located outside of ISIM on the connecting truss. The Scientific Instrument Controls (SIC) for all instruments are located in the Satellite Support Module (SSM).

Figure 2.5-1 shows a functional block diagram of all instruments within the spacecraft context, with the main instrument and spacecraft components and important thermal and physical constraints.

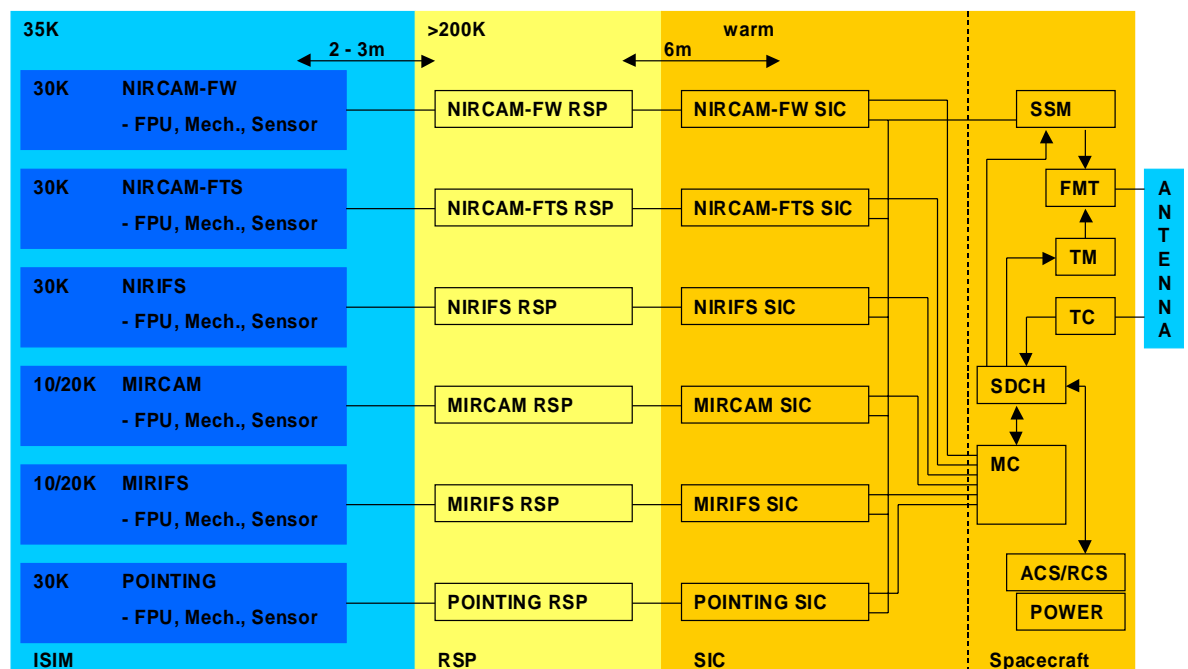


Figure 2.5-1: Overall functional block diagram

Located on the connecting truss are the Remote Signal Processing electronics for each instrument. An RSP includes the following components:

- Interface to instrument SIC: FPU parameters and control, Sensor data, Main power, mechanism control

- Internal RSP clock, control and power generation
- FPU bias and clock generation
- Analog signal processing of FPU data: Preamplifier, filters, impedance matching

Analog Digital Converter

- Parallel/Serial Conversion with high data rate link
- Mechanism control, may include sensors for position indication
- Sensor electronics (ADC and serial data link)

The instrument FPU/RSP's are controlled by the Scientific Instrument Controllers (SIC's). An SIC performs the following tasks:

- Spacecraft interface for reception and processing of Mission Controller (MC) commands and parameters.
- RSP control (parameters for image acquisition)
- Mechanism control
- Reception of digital science data
- Science data processing and data compression
- Science data storage

In the following more detailed functional block diagrams and descriptions for each individual instrument are shown (Figure 2.5-2 to Figure 2.5-7):

NIRCAM Filter Wheel

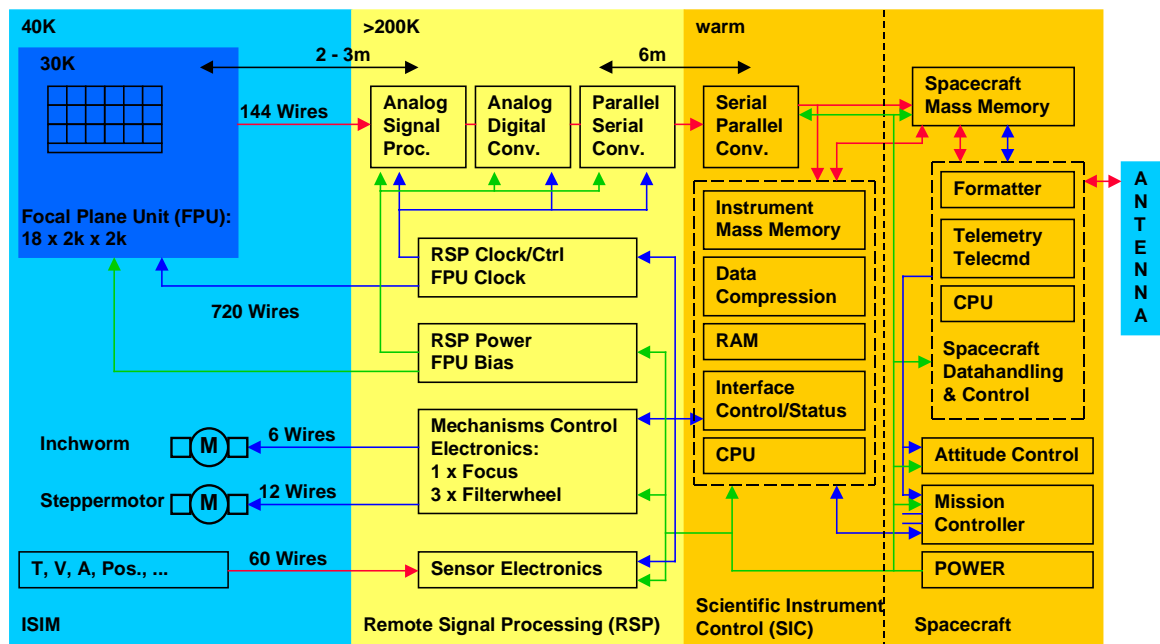


Figure 2.5-2: NIRCAM Filter Wheel functional block diagram

NIRCAM FW components located within ISIM are:

- Focal Plane Unit (FPU) at 30K, consisting of the SCA (Sensor-Chip-Assembly = detector + multiplexer)
- Stepper motor for filter wheel selection with no dissipation in power-off condition
- Actuator for refocus adjustment with no dissipation in power-off condition
- Hold-down and release mechanism for refocus mirror with no dissipation in power-off condition
- Sensors for temperature

NIRCAM FTS

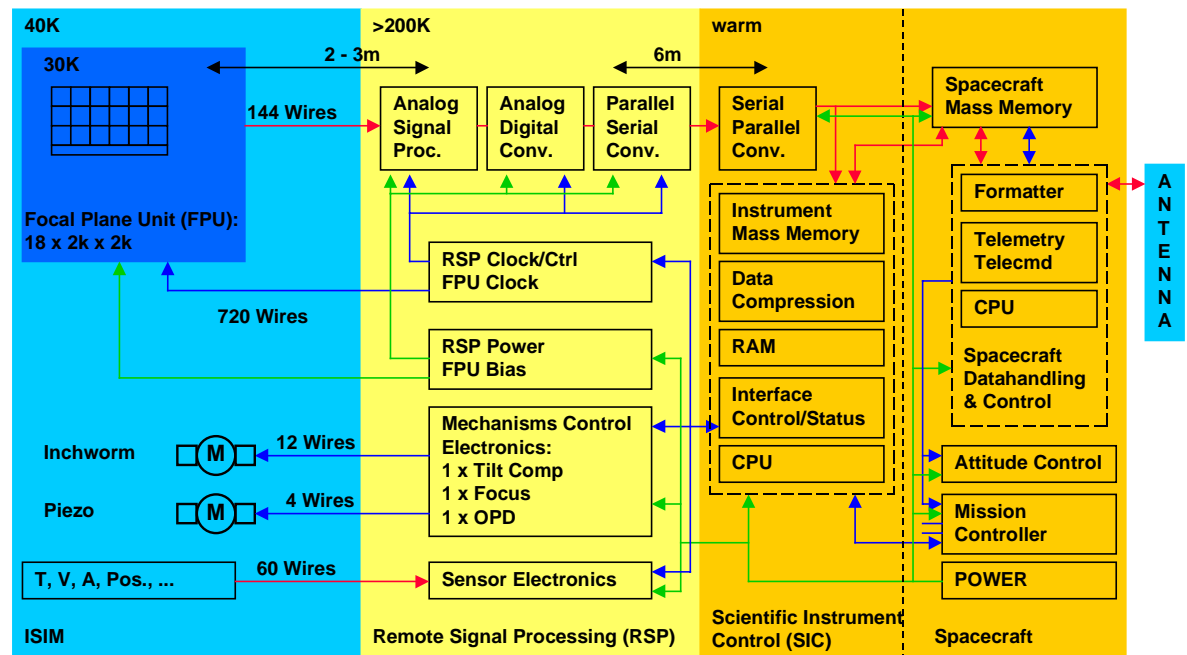


Figure 2.5-3: NIRCAM FTS functional block diagram

NIRCAM FTS components located within ISIM are:

- Focal Plane Unit (FPU) at 30K, consisting of the SCA (Sensor-Chip-Assembly = detector + multiplexer)
- Piezo driven motor for OPD movement
- Actuator for refocus adjustment with no dissipation in power-off condition
- Actuator for tilt compensation mechanism
- Hold-down and release mechanism for refocus mirror with no dissipation in power-off condition
- Sensors for temperature

IFMOS

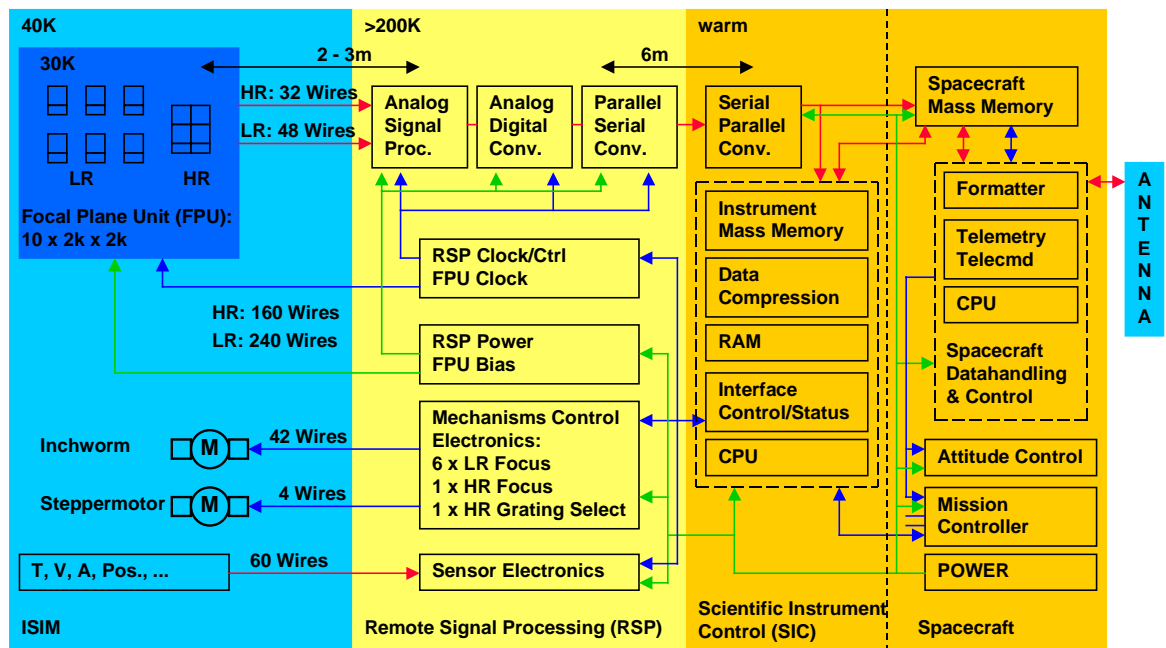


Figure 2.5-4: IFMOS functional block diagram

IFMOS components located within ISIM are:

- Focal Plane Unit (FPU) at 30K, consisting of the SCA (Sensor-Chip-Assembly = detector + multiplexer)
- Stepper motor for grating change mechanism with no dissipation in power-off condition
- Actuator for refocus adjustment with no dissipation in power-off condition
- Hold-down and release mechanism for refocus mirror with no dissipation in power-off condition
- Sensors for temperature

MIRCAM

The MIRCAM components located within ISIM are:

- Focal Plane Unit (FPU) at 8K, consisting of the SCA's (Sensor-Chip-Assembly = detector + multiplexer) for the 5-10 μ m and the 10-30 μ m regions.
- Stepper motor for filter wheel selection with no dissipation in power-off condition
- Sensors for temperature

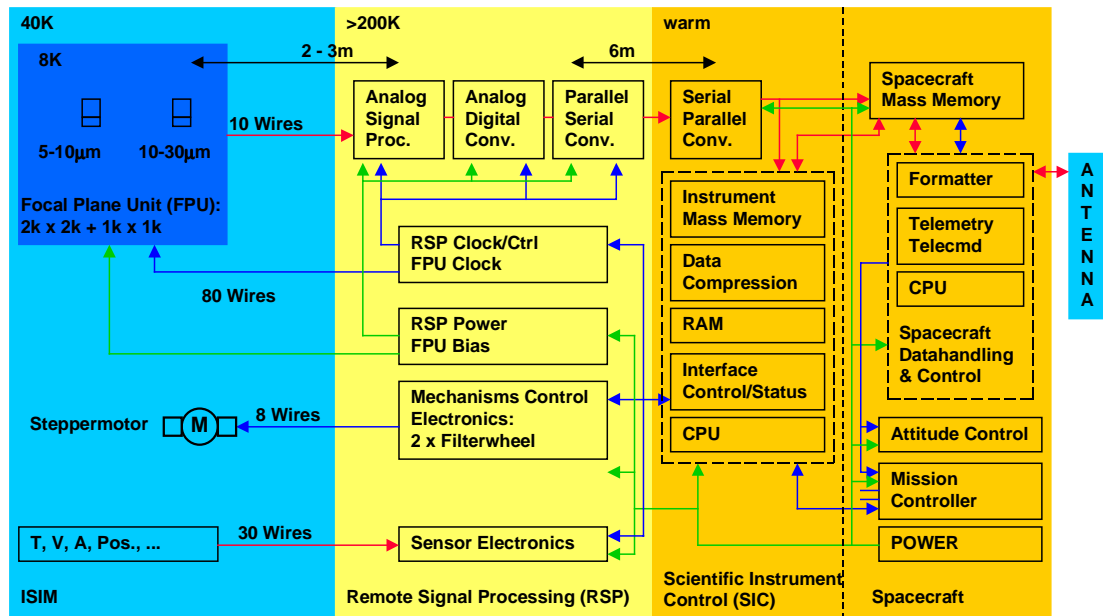


Figure 2.5-5: MIRCAM functional block diagram

MIRIFS

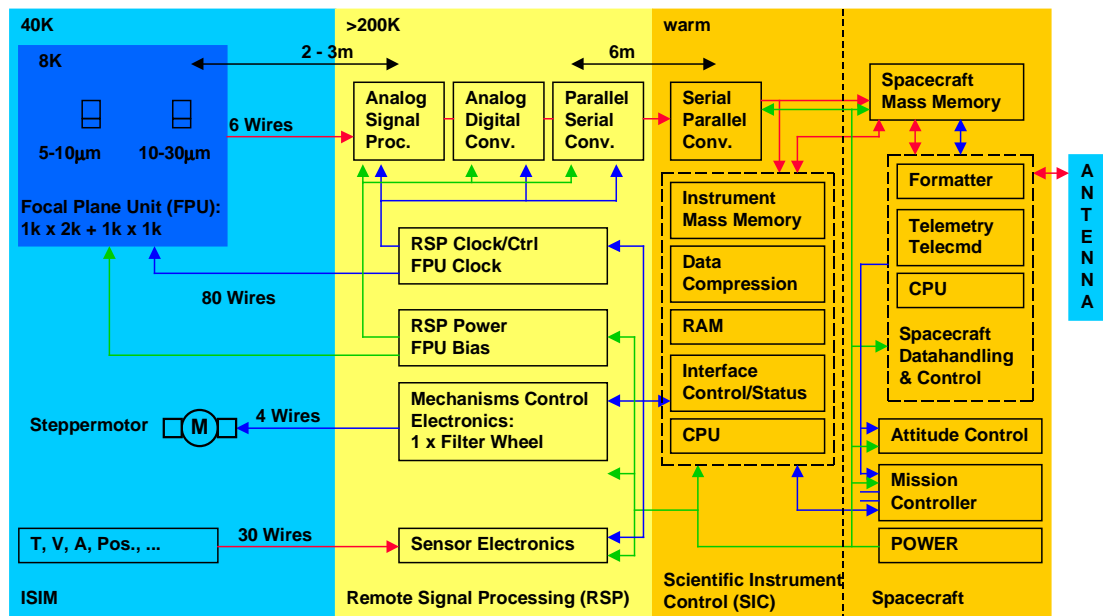


Figure 2.5-6: MIRIFS functional block diagram

MIRIFS components located within ISIM are:

- Focal Plane Unit (FPU) at 8K, consisting of the SCA's (Sensor-Chip-Assembly = detector + multiplexer) for the 5-10µm and the 10-30µm regions.
- Stepper motor for filter wheel selection with no dissipation in power-off condition
- Sensors for temperature

2.5.2 Analog Signal Processing Design Trades

The design and the arrangement of signal processing components depends strongly on the electrical, mechanical, thermal and functional instrument requirements (i.e Signal/Noise) and on available component technology. These stringent requirements may require a specific NGST development. An overview of the design trades is shown in Figure 2.5-8.

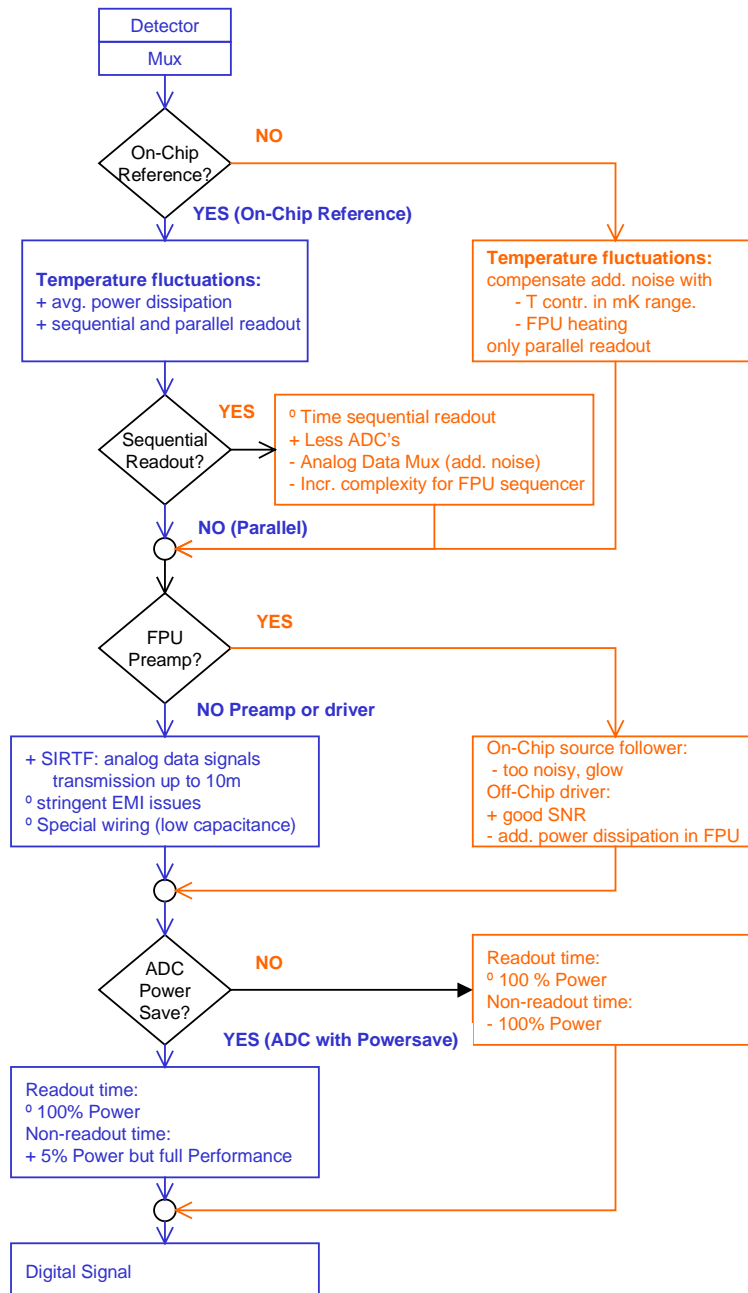


Figure 2.5-7: Analog Signal Processing Design Trades and Baseline

SCA on-chip reference

On-board signal processing design is based on SCA testing/characterization and experience with current devices. But long integration times (~1000 sec) and in-space operation may exhibit new SCA behavior when NGST is in orbit.

Long integration times require in general a temperature stability of the SCA in the milliKelvin range. Otherwise the thermal fluctuations result in additional read noise. In addition in an integration/readout sequence of an SCA power is only dissipated in the readout phase. In a sequence of nondestructive readouts the SCA experiences a heatup and cooling cycling resulting in additional thermal fluctuations. There are two solutions for thermal fluctuation reduction/elimination:

SCA heating and thermal control:

Heating of the SCA during the time when there is no readout and thermal control in the milliKelvin range:

- Single data output.
- This method requires a more complicated cooling concept and it will be difficult to provide milliKelvin range control at the FPU within NGST.
- Because of heating, power is constantly dissipated even during non-readout time with the same amount as the SCA.

Integration of an on-chip reference in the SCA:

- + Reference output exhibits same thermal fluctuations as data output: Differential processing eliminates fluctuations.
- + No milliKelvin range thermal control required.
- + No heating during non-readout time therefore dissipation can be averaged.

Differential output requires double wires with differential receiver.

Baseline:

The on-chip reference provides significant advantages in terms of thermal control requirements, heat dissipation and S/N performance. It can be anticipated, that it will be available on NGST type SCA's.

Parallel/Sequential readout

In general the time for reading out an SCA array is shorter than the time between readouts (therefore also power dissipation averaging). This can also be utilized for sequential readout of a number of arrays. If for example the time between readouts is 15 sec and the time for an array readout is 5 sec, the first third of the arrays could be read out in the time 0-5sec, the second third in the time 5-10sec and the last third in the time 10-15sec. On the remote signal processing side, a multiplexer is inserted into the signal processing chain with a multiplexer ratio of 3:1. The number of ADC's can be reduced to a third.

With parallel readout all arrays are read out at the same time, in the example within the 0-5sec time frame.

Sequential readout:

- + Parts of the remote signal processing chain can be reduced, which saves number of components and power, which is usually high for ADC's.
- Increased complexity for bias and clock logic
- Additional Analog Data Multiplexer in remote signal processing chain may be significant noise source.
- Continuous data flow with reduced data rate

Parallel readout:

- + Synchronous readout (low crosstalk)
- + No analog data multiplexer in remote signal processing chain
- Minimum complexity for bias and clock logic
- Data is generated in bursts with high momentary data rate

Complete signal processing chain per output (one ADC per output)

Baseline:

Parallel readout: Emphasis of all instruments signal processing is on radiometric performance, therefore the performance gain of parallel readout over sequential readout outweighs the disadvantages.

FPU Preamplifier

The signal processing electronics is placed a large distance from the FPU (several meters). In a general application the analog data signals are amplified for transmission over this distance, mainly for EMI reasons. Preamplifiers in FPU proximity dissipate power and therefore increase the power budget within ISIM. SCA manufacturers do place source followers (line drivers) on the SCA. The different implementations may have the following drawbacks, which very much depend on the chosen SCA:

- On-chip source follower is of unit-cell size: due to small geometry this is an additional noise source, which far exceeds the read noise requirements
- On-chip source follower glow: either thermal or visible, which results in location depend dark current increase, in general exceeds requirements

Alternatives are:

- On-chip source follower significantly larger than unit-cell size, which meets the read noise requirements
- Off-chip source follower in very close proximity to SCA

Baseline:

The source followers can drive a couple hundred picoFarad and with proper EMI considerations and harness design, transmission over a long distance is possible as shown with the SIRTf (NASA) instrument. This will most likely be sufficient for a camera type instruments, which are shot noise limited. But for instruments like IFMOS, which is read-noise limited, even with proper EMI design, an additional preamplifier may be required to meet the S/N requirements. Additional estimated power dissipation is 5mW per output (double in case of differential output).

The source follower is in general included in the power dissipation parameters given for the SCA.

ADC with Power Save Mode

During non-readout time, the SCA does not dissipate power, which is important for the average power budget within ISIM. With parallel readout, a large number of remote signal processing components are required, leading to high dissipation in the ISIM vicinity. One of the largest contributors are the ADC's. In order to meet the performance requirements continuous operation, even during non-readout time, is required. For that reason, ADC's devices with a power save mode should be considered. Devices are available with the following modes:

- Sleep mode: Most ADC components are powered off. On power-on critical components may not have stable operational performance, introducing a noise factor.
- Nap mode: Critical ADC components are still powered on (like reference), non critical are powered off. ADC operation meets performance.

Baseline:

Implementation of a 16 Bit ADC (max. 200kHz conversion rate) with power saving modes. In nap mode about 5% of full power is dissipated.

2.5.3 FPU Readout Scheme

The readout scheme is designed for a multisampling method with on-board flexibility. An up-the-ramp sampling method is used as a baseline (see also Science Data Processing section).

FPU Configurations

Table 2.5-1 shows the FPU configurations. The detectors are assembled with butted modules, either be based on 2kx2k or 1kx1k SCA's depending on availability. Either SCA will have one output per 1kx1k array, resulting in a high output count of for example 72 outputs for a NIRCAM instrument.

The maximum readout rate is 200 kHz with a power dissipation of 1mW per 1K x 1K module.

The SCA clocking logic (sequencer) allows for non-destructive readout and subarray addressing (required for tracking tasks).

Instrument	Detector Format	Module Size	Nr. of Modules	Nr. Outputs/ Module	Total Nr. of Outputs	Power/Module [mW]
NIRCAM-FW	12k x 6k	2k x 2k	18	4	72	4
NIRCAM-FTS	12k x 6k	2k x 2k	18	4	72	4
IFMOS	10 x 2k x 2k	2k x 2k	10	4	40	4
MIRCAM 5-10 μ m	2k x 2k	1k x 1k	4	1	4	1
MIRCAM 10-28 μ m	1k x 1k	1k x 1k	1	1	1	1
MIRIFS 5-10 μ m	1k x 2k	1k x 1k	2	1	2	1
MIRIFS 10-28 μ m	1k x 1k	1k x 1k	1	1	1	1
Pointing Sensor	3 x 2k x 2k	2k x 2k	3	4	12	4

Table 2.5-1: FPU configurations

Up-the-ramp Sampling Method

Observations will be several hours, but a long exposure is split-up into exposure frames of 1000 sec length. Due to effects like cosmic ray impacts, read noise reduction, a 1000 sec frame is again split into subframes.

At the beginning of a frame at t=0, the SCA's are reset and then n non-destructive readouts are performed. A SCA reset is again performed at the next 1000 sec frame start. In the following diagram and for the corresponding budget calculations n=64.

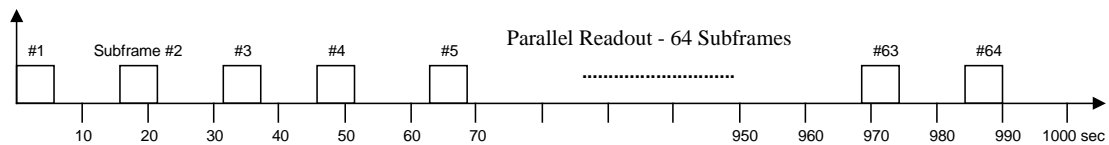


Figure 2.5-8: Timing Diagram

The timing diagram in Figure 2.5-9 shows an even distribution of 64 subframes over the whole exposure time of 1000 sec. One readout takes:

$$1024 \times 1024 \text{ [pixel/output]} \times 1/200000 \text{ [sec/pixel]} = 5.24 \text{ [sec/output]}$$

The cycle time is

$$1000[\text{sec}] / 64 = 15.6 \text{ [sec]}$$

Power is only dissipated during the readout period, which is 5.24 sec. The average power dissipation therefore is

$$5.24/15.6 = 0.33 \sim 1/3 \text{ of the continuous power dissipation}$$

Reduction of the readout rate from 200kHz to for example 100kHz will have the following effects:

- power dissipation in FPU is reduced by factor of 2, because SCA power is a factor of readout rate and much less array size.
- bandwidth requirements for data transmission from FPU to RSP are reduced
- RSP signal processing component requirements because of lower bandwidth are accordingly reduced
- lower burst data rate

The FPU bias and clocking electronics in the RSP should be designed to allow a flexible readout scheme, which can be adapted to experience gained during operation. For example as mentioned previously SCA characteristics may surface in-orbit and optimization of cosmic ray removal algorithms in-orbit may be required.

2.5.4 Signal Processing Power Budget and Harness Size

Power and Wiring Parameters depend on the final component selection. At this stage only estimates can be given.

In terms of SCA power, the current 1mW per 1K x 1K array can be considered an upper limit. The number of wires for the SCA includes redundancy considerations, which prevents loss of more than 1 Mpixel from a single point failure.

For the ADC's the estimate is 200mW per converter with a reduction to 5% in nap mode.

Very critical is the harness design in terms of impedance and EMI for the analog data signals (shielded, differential), especially when no preamplifier is used in SCA proximity.

RSP power generation is very critical in terms of noise, possibly linear converters with low efficiency are required.

Table 2.5-2 shows the power and Table 2.5-3 the wire estimates for the FPU, mechanics, sensors in ISIM and in RSP.

Instrument	FPU		RSP					
	SCA [mW] Cont./Avg.	Mech. [mW]	ASP [W]	ADC [W] Cont./ Powersave	Clock/ Ctrl [W] (2)	Bias/ Power (2)	Mech. Ctrl [W]	Sensor Electr. [W]
NIRCAM-FW	72/25	(1)	2.2	14.4/5.4	2	8	0.5	0.1
NIRCAM-FTS	72/25	(1)	2.2	14.4/5.4	2	8	0.5	0.1
IFMOS	40/14	(1)	1.2	8/3	1	5	1	0.1
MIRCAM	4+1/1.4+0.35	(1)	0.15	1.0/0.4	0.2	0.5	0.5	0.1
MIRIFS	2+1/0.7+0.35	(1)	0.09	0.6/0.2	0.2	0.5	0.2	0.1
Pointing Sensor	12	(1)	0.36	2.4	0.5	1	-	0.1

(1) No continuous operation

(2) Rough estimates, depend on device complexity and technology

Table 2.5-2: Power estimation

Instrument	Data Signals (1)	Clock/Ctrl/ Bias (2)	Mechanisms (3)	Sensors
NIRCAM-FW	144	720	18	60
NIRCAM-FTS	144	720	16	60
IFMOS	80	400	46	60
MIRCAM	10	80	8	30
MIRIFS	6	80	4	30
Pointing Sensor	24	120	-	20

(1) Shielded (Differential), low impedance (~100pf), 0.1mm, EMI !!!

(2) 0.1 mm

(3) < 0.5 mm

Table 2.5-3: Harness size estimation

2.6 Signal Processing

Observations with ISIS will be several hours, but are split-up into subframes of 1000 sec length. Non-destructive readout is standard practice with IR detectors and provides several advantages for NGST operations, like up-the-ramp sampling.

2.6.1 *Up-the-ramp sampling:*

During a long-term exposure the SCA is read out periodically. This could be a number of closely spaced readouts at the beginning of the exposure and the same number of closely spaced readouts towards the end of the exposure (Fowler sampling) or a number of readouts spaced evenly throughout the exposure. The readout scheme may also be adapted to take certain SCA, or instrument characteristics into consideration. After collection of the n subimages, they are combined to a final image. This can be accomplished by transmitting all subimages to the ground, or by combining them on-board to a final image. In the following an evenly spaced readout scheme is considered baseline. Three major advantages for NGST of up-the-ramp sampling are described as follows:

Dynamic range expansion

During a longterm exposure (~1000sec) objects with different magnitude will be imaged. While some object may barely be above the S/N limit, bright objects will quickly reach the SCA full well capacity. A single long exposure image would lose all detail of bright objects in this case. Up-the-ramp sampling monitors the 'brightness' of the individual pixels and terminates the integration when full well capacity is reached. Based on the integration slope, a final exposure value is extrapolated (Figure 2.6-1).

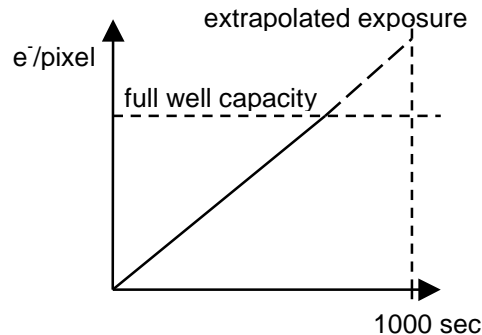


Figure 2.6-1: *Dynamic range expansion of up-the-ramp sampling scheme.*

Cosmic Ray Correction

Cosmic ray events can be estimated for NGST SCA based on HST experience. The impact rate is about 4 events per cm^2 and sec. On the average ~ 5 pixels affected with a pixel size of $18.5 \mu\text{m}$. The peak impact has an affect of a 10000 e^- change in charge

(Figure 2.6-2). In case of a 2k x 2k detector (2048 pixel x 0.00185 cm)² x 4 x 5 = 287 pixel/sec are affected. This is a significant amount, because 1 % of the SCA is affected after just 146 s exposure time. In case of a 1000 sec total exposure, the amount of pixels affected is not tolerable for scientific evaluation.

Pixel charge changes proportional with the exposure time, when illuminated by constant source => constant slope. Intensity deviations can then be attributed to cosmic ray effects. Interrogation of the slope of each pixel over a number of subimages identifies a cosmic ray impact and allows its correction. This operation is performed on-board and the corresponding pixels are identified by applying a correction tag and statistics information.

In reality the correction algorithm will be more complex, because it has take global and local frame parameters, systematic errors and calibration parameters into consideration. Also the cosmic ray impact is not a perfect step function, time varying effects are observed. It is important to analyse the cosmic ray impact nature to establish a suitable correction algorithm.

It is estimated, that the cosmic ray removal algorithm can reduce the number of affected pixels to <<1%.

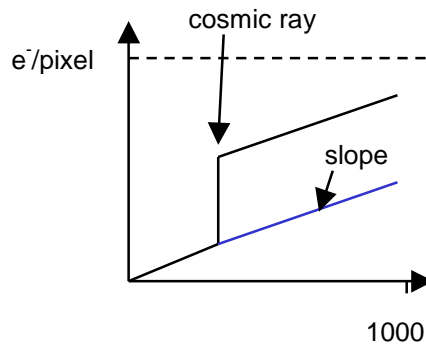


Figure 2.6-2: Cosmic ray correction with up-the-ramp sampling scheme.

The implementation and complexity of the algorithm depend strongly on on-board processing power capability and availability and accessibility of memory (local and mass storage).

Readout Noise Reduction

Each individual readout is affected by noise. Taking a number of readouts, calculating the slope and a final exposure, the readout noise in the final image is less than the readout noise in a single exposure of the same time, simply by statistics. Readout noise reduction depends on the sampling scheme, but is vital for read noise limited systems like IFMOS and NIRCAM-FTS. Figure 2.6-3 represents the error bars based on readout noise for each subimage, with the straight line fit through the data points leading the final exposure value with overall lower readout noise.

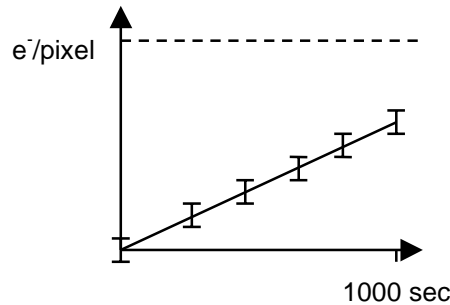


Figure 2.6-3: Readout noise reduction with up-the-ramp sampling scheme

2.6.2 NIRCAM FTS Signal Processing

The NIRCAM FTS instrument works in a camera mode and an interferometer mode with different data processing:

In the camera mode the operation is identical to the NIRCAM FW with parallel readout und Up-the-Ramp Sampling.

In interferometer mode mechanical motion is introduced. In order to acquire a complete spectrogram the total integration time can be hours depending on radiometric requirements. An example for spectrogram acquisition could be as follows:

Sampling is performed over path length of 0.1mm with 300 steps. The total integration time is 10 hours. In this case the step time is $36000 \text{ s} / 300 \text{ steps}$, which is 120 s exposure time per step. Up-the-Ramp Sampling, as mentioned later, is utilized with $N=8$ non destructive readout samples at each step (15 sec integration time). At the start of each new step a SCA reset is performed.

During the 120 step exposure time, about 0.7% of pixels will experience cosmic ray impact. Cosmic ray correction in interferometer mode is different and probably less complex as in camera mode. Up-the-ramp sampling can utilize neighboring step information and apply thresholding based on a priori spectrogram knowledge into consideration. In addition Fourier transform of a spike contributes only a slight DC offset.

2.6.3 Data Processing Requirements

Processor Requirements

Because of the large amounts of data collected on-board with up-the-ramp sampling and the limited downlink rate, the main on-board processing task will be up-the-ramp sampling processing, including readout noise reduction, dynamic range expansion and cosmic ray removal. As already described, the final requirements cannot at this stage be established. Even then, adaptation to in-flight experience should be possible with a flexible on-board processing architecture with margins.

In order to get an estimate for the magnitude of processing requirements a simple cosmic ray removal algorithm is investigated. It assumes a step function without any of the additional time varying effects and other system parameters. In addition a stable image over the total integration time is assumed (no correction for image jitter or rotation). Figure 2.6-4 shows a flow chart of such a simple algorithm, which calculates the intensity change from frame to frame, identifies cosmic ray events by evaluating the statistics of the difference values. Unaffected subimages are then combined by slope fitting and matching. From these values the final 1000 sec intensity is calculated.

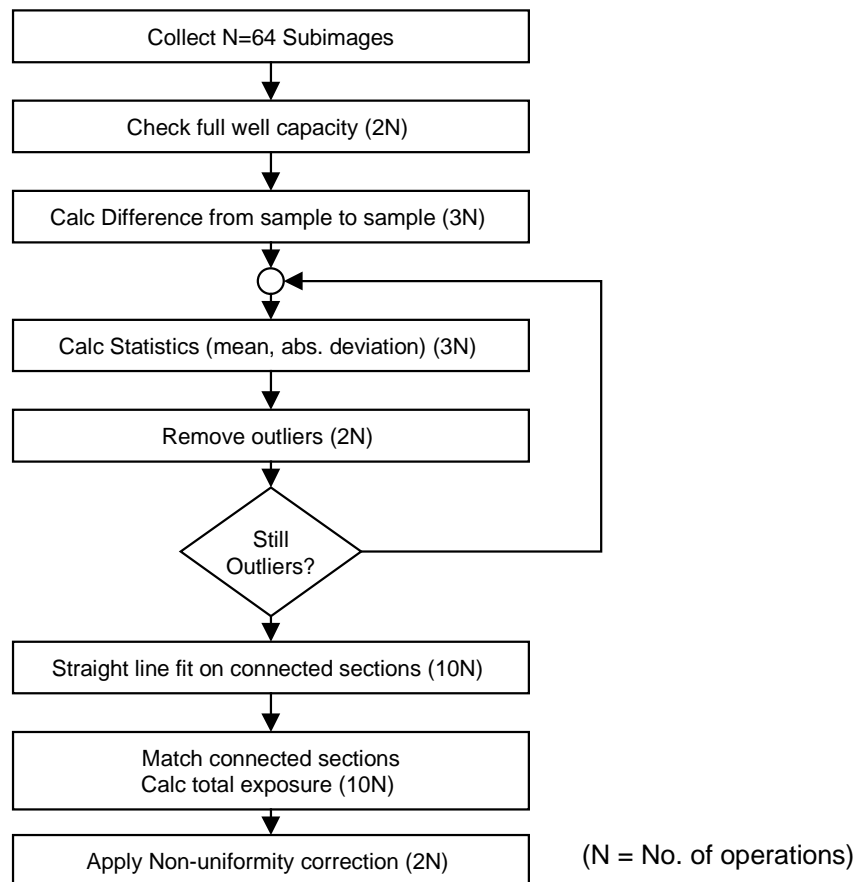


Figure 2.6-4: Simplified Cosmic Ray Removal Algorithm

As an example, with IFMOS 42 Mpixel (based on 64 Subimages) need to be processed. Assuming that the processing needs to be performed within one total exposure time of 1000 sec, a single pixel needs to be processed in 23 ms. The simplified example in Fig. 2.6-4 requires a minimum of $32 \cdot N = 32 \cdot 64 \sim 2000$ instructions performed per pixel. In order to process 42 Mpixel in 1000 sec at 2000 instructions per pixel, a processing rate of 84 Mips is minimum. This is feasible with current processor technology with single CPU's or a small number of DSP's. Table 2.6-1 shows the processing requirements for all instruments.

With additional ‘real time’ processing requirements for other extensive processing tasks, (complex cosmic ray correction, misalignment matching, super-resolution, ...) the required processing resources may become critical.

Storage and Data Rates

The expected maximum spacecraft downlink rate is 1.6 Mbps with a mass memory capacity of about 40 Gbit.

For determination of storage requirements the following is assumed:

- up-the-ramp sampling with 1000 sec total exposure and $N = 64$ subframes for cameras and $N = 8$ for FTS
- all subframes need to be stored in a local mass memory for post-processing
- double memory for current frame data collection and prev. frame data processing
- 1 additional byte per pixel overhead for info (status, time, correction tags, etc.)

Instrument	subframe size [Mpixel]	instrument mass storage size [Gbit]	processed frame size; CR = 2 [Gbit]	processor requirements [Mips]
NIRCAM-FW	75.5	155	0.9	150
IPTS Camera	75.5	155	0.9	150
IPTS Interferometer	75.5	48.3	0.9	150
IFMOS	42.0	86.4	0.5	84
MIRCAM	5.3	10.8	0.05	11
MIRIFS	3.2	6.5	0.04	7

Table 2.6-1: Storage and processor requirements

The Table 2.6-1 shows that operation of the instruments needs to be efficiently managed because of the limited spacecraft downlink capacity. Quasi-lossless compression methods can significantly reduce these budget values.

2.7 Critical Areas and Recommended Development Activities

2.7.1 Generic Instrument Hardware Breakdown

Figure 2.7-1 shows a generic HW breakdown that can be applied to all investigated instruments. The optics subsystem is instrument specific and not further detailed. The shaded boxes indicate critical subsystems or subsystems containing critical elements; corresponding details are provided in the following chapter.

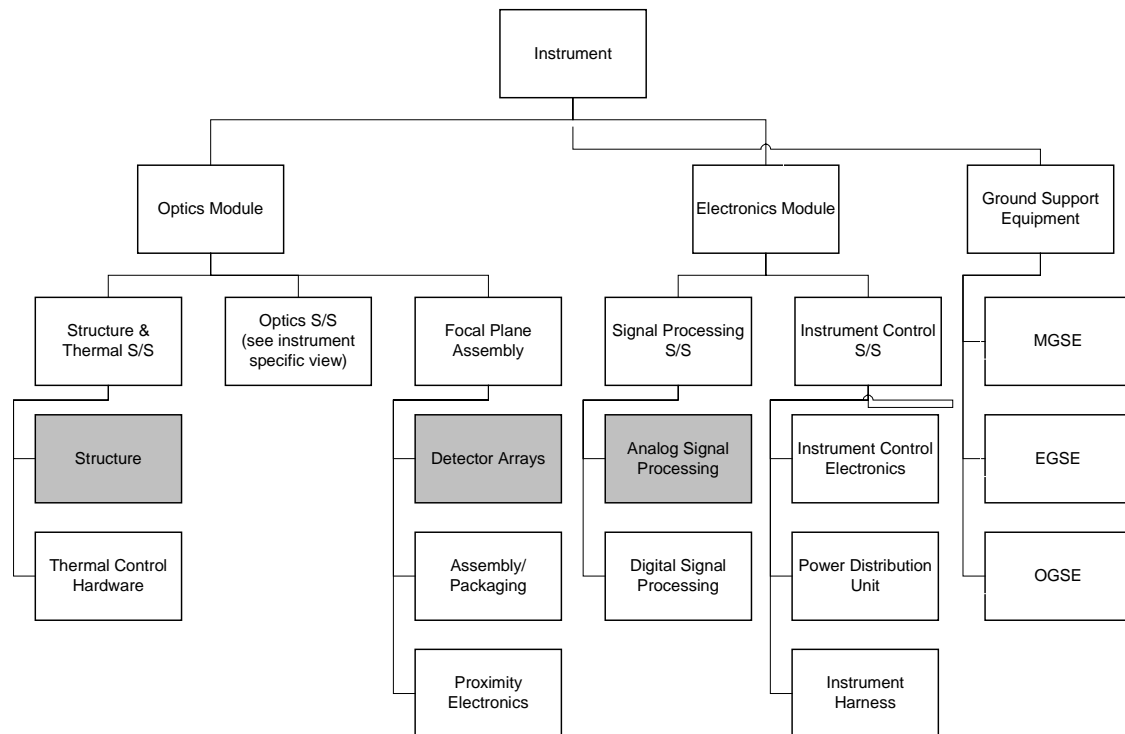


Figure 2.7-1: Instrument Hardware Breakdown; shaded areas indicate critical subsystems.

2.7.2 Critical Areas and Technology Requirements

Potential criticalities to be considered during the development of the instruments are

- items whose failing may affect the satellite performance or survival probability
- single point failures and non-redundant major elements
- items whose failing/degradation may affect the instrument performance
- items not previously space qualified
- items with exceptional process sensitivity and long lead items

The critical areas of the investigated instruments are mainly concerned with the last two items, i.e. structure materials and subsystems which contain new technologies or technologies of expected long development duration.

Critical Areas and Risks

The following Table 2.7-1 provides an overview of potential critical technologies, which are common to all investigated instruments. These technologies need to be identified in an early stage of the project to allow definition of a dedicated technology development program in order to reduce the development risks of the project.

Subsystem	Critical area	Comments
structure	large dimensions: mass and stiffness critical, sensitive to thermal gradients	Al: performance critical; Be: handling and cost critical; C/SiC: new technology
actuators	lifetime, performance at 30K	on-going developments for M1
detector arrays, analog processing	performance (low dark current) and butting of large arrays	on-going developments: recent tests on InSb and Si:As detectors show promising performance
	long distance data transmission w/o preamp: EMI may introduce noise	locate pre-amps for HR instruments close to detectors (thermal load!)
schedule	NASA compatible schedule is rather short	select adequate model philosophy

Table 2.7-1: Potential critical areas common to all instruments

The listed items are considered of high criticality and require an early demonstration of feasibility. Any failure of the prove of concept of these items will require a revision of the conceptual design or even the change towards a completely new design concept. The short development schedule will require careful task planning and additional design and/or analysis effort in order to meet the delivery dates.

One of the most critical areas identified in this context is the proposed C/SiC material for the instrument structure and possibly optical components. This promising material has been developed in the early 1990s and has been used in the OERSTED project. For SEVIRI a 60 cm mirror and a 2 m structure for ground calibration purposes have been developed, built and tested successfully, the mirror under qualification loads. Further use of this material in space projects is currently under discussion. The criticality of this material is related to the unknown material parameters at the foreseen low temperature operating conditions and to the lack of experience with corresponding low temperature interface connections.

Another area of potential criticality concerns the **signal processing**:

- up-the-ramp sampling and image processing requires large instrument mass storage => possibly reduce amount of sub-samples per 1000 sec

- in-orbit instrument characteristics (esp. detector arrays) are difficult to simulate and may change with time => requires flexible image processing concept with SW upgrading capability

However, these items are of lower criticality grade and can be treated within the standard engineering tasks.

2.7.3 **Recommended Development Activities**

In order to minimize the development risks certain technology development activities are recommended. Some of these activities are essential for the *prove of concept* and the results should be available prior to further instrument design detailing (ideally prior to Phase A). In the development schedule of the different instruments these activities are referred to as **Technology Pre-Developments**.

Further development activities are aiming for gain of experience with the new technologies. These activities should be started during Phase A and the results should ideally be available at begin of the detailed design phase (Phase B). In the instrument development schedule these activities are referred to as **Technology Developments**.

For each of these activities, the following technology development activities are proposed:

1. review of existing technologies and preliminary design
2. manufacturing of a representative unit
3. verification of performance prior to and after environmental tests, at ambient and at operating conditions

Verification of C/SiC Material for Structural and Optical Components

C/SiC has been proposed as baseline material for the instruments resulting in high structural and thermal stability and low mass. For NGST use the following parameters need to be verified:

- optical figure of C/SiC mirrors at RT and operational temperature as well as after vibration testing
- straylight properties (surface quality) for large mirrors
- stability of C/SiC interface connections (with C/SiC and other materials)

The following technology pre-development activities are considered mandatory to ensure the C/SiC material applicability for low temperature:

1. Measurement of C/SiC physical parameters down to about 20K (CTE, thermal conductance, thermal capacitance, etc.)

Duration: 6 months

2. Behavior of C/SiC mirror surface at low temperatures:
 - manufacturing of test mirror with a typical size (about 30cm)
 - optical performance measurements at ambient, LN2 and ~ 20 K

Duration: 12 months

The following additional technology developments are aiming to gain further experience with this material:

3. Joining of interface elements:

- manufacturing of test plates with selected candidate joining methods
- load and stability tests at RT, thermo-stability at LN2 and ~ 20 K

Duration: 8 months

4. Opto-mechanical performance at low temperatures:

- manufacturing of test bench or cube (IFMOS) with typical instrument dimensions
- opto-mechanical performance from ambient down to LN2 (extrapolation to 30K)

Duration: 12 months.

Technology Development Activities at System Level

There are other technology verification activities which are considered necessary, especially the development of the detectors and mechanisms for refocusing. But these technologies will be needed for other NGST hardware units as well and it is assumed that they will be developed under NASA contracts on system level (development activities are on-going).

2.7.4 Technology Development Roadmap

The technology development roadmap for common critical technologies is depicted in Figure 2.7-2 below. It shows the main critical hardware elements, to be developed in an early stage of the project:

- C/SiC material at cryogenic conditions
- actuators/mechanisms
- low noise detectors, butting of large arrays

It is assumed that the detectors and mechanisms (for optics refocusing) for NGST will be developed on system level, since these technologies are not instrument specific and will be required for other NGST space hardware units as well.

The instrument specific recommended technology development activities are summarized in the box “critical optical technologies”, and are detailed in the corresponding instrument papers.

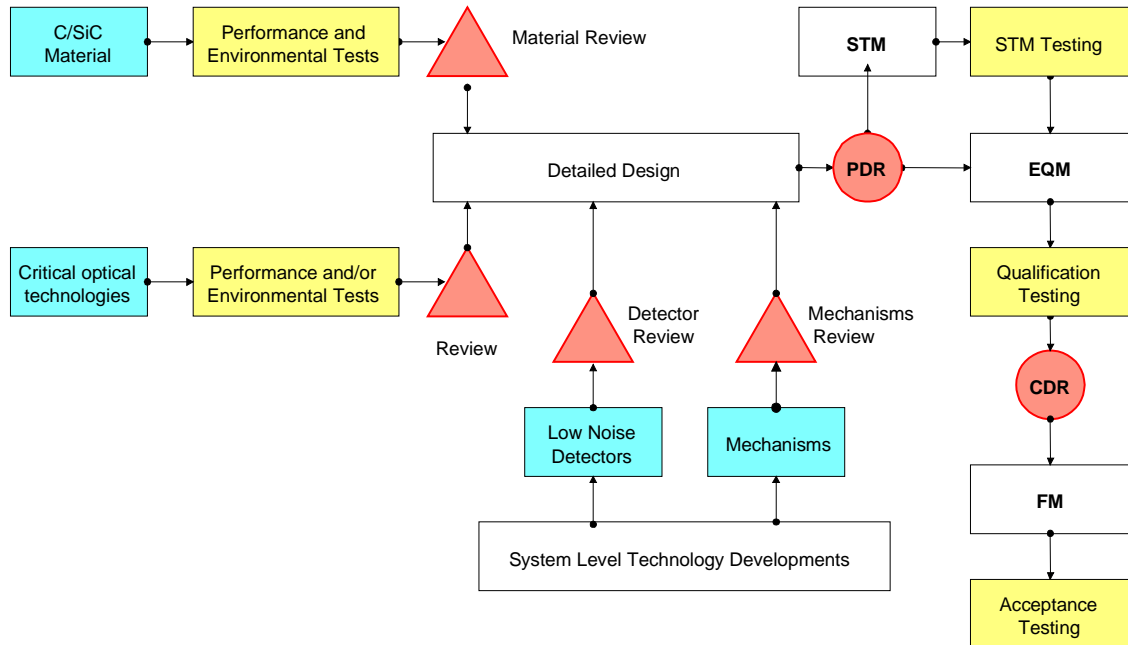


Figure 2.7-2: Technology Development Roadmap

2.8 Development Planning for Phases B and C/D

The development planning for phases B and C/D will be treated in the corresponding instrument papers.

3 REFERENCES

- /1/ “Study of Payload Suite and Telescope for NGST”,
ESTEC/Contract no. 13111/98/NL/MS
- /2/ Statement of Work for “Study of Payload Suite and Telescope for NGST”,
PF-NGST-SOW-002, Issue 1, 24-Apr-98
- /3/ “Study of a Multi-Object/Integral Field Spectrograph”,
AO/1-3406/98/NL/MS